Random time step probabilistic methods for uncertainty quantification in chaotic and geometric numerical integration

Assyr Abdulle* Giacomo Garegnani†

Abstract

A novel probabilistic numerical method for quantifying the uncertainty induced by the time integration of ordinary differential equations (ODEs) is introduced. Departing from the classical strategy to randomize ODE solvers by adding a random forcing term, we show that a probability measure over the numerical solution of ODEs can be obtained by introducing suitable random time-steps in a classical time integrator. This intrinsic randomization allows for the conservation of geometric properties of the underlying deterministic integrator such as mass conservation, symplecticity or conservation of first integrals. Weak and mean-square convergence analysis are derived. We also analyse the convergence of the Monte Carlo estimator for the proposed random time step method and show that the measure obtained with repeated sampling converges in the mean-square sense independently of the number of samples. Numerical examples including chaotic Hamiltonian systems, chemical reactions and Bayesian inferential problems illustrate the accuracy, robustness and versatility of our probabilistic numerical method.

AMS subject classifications. 65C30, 65F15, 65L09.

Keywords. Probabilistic methods for ODEs, random time steps, uncertainty quantification, chaotic systems, geometric integration, inverse problems.

1 Introduction

A variety of methods for integrating ordinary differential equations (ODEs) has been studied in the last decades, [9–11], with an emphasis on building accurate and stable deterministic approximations of the exact solution. In general, these methods are based on a time discretisation on which the solution of the ODE is approximated via an iterative deterministic algorithm. Given a time step h, which indicates the refinement of the discretisation, all these methods provide a point value for the approximation of the solution and guarantee that in the asymptotic limit of $h \to 0$ the numerical approximation will coincide with the exact solution. However, for some problems such as chaotic systems or inference problems having a distributional solution can help to quantify the uncertainty introduced by the numerical discretisation without invoking the asymptotic limit $h \to 0$.

In recent years, probabilistic numerical methods for differential equations have been proposed [4,6,21] in order to quantify the uncertainty introduced by the time discretisation in a statistical manner. In general, these methods proceed iteratively to establish a probability measure over the numerical solution, thus providing a richer information than a single point value. In particular, probabilistic solvers offer a quantitative characterisation of late time errors by tuning the noise introduced by the method according to the accuracy of the solver. In this way, it is possible to obtain a reliable approach for capturing the sensitivity of the solution to numerical error, while transferring the convergence properties of classical deterministic integrators to the introduced probability measure in a consistent manner.

*Mathematics Section, École Polytechnique Fédérale de Lausanne (assyr.abdulle@epfl.ch)
†Mathematics Section, École Polytechnique Fédérale de Lausanne (giacomo.garegnani@epfl.ch)

In the following, we will first show three examples motivating the probabilistic approach, and then present the main contributions of this work.

1.1 Motivating examples

Probabilistic integrators for ODEs do not provide more accurate solutions than classical deterministic methods nor are they computationally cheaper. Nevertheless, they can be useful in a variety of different problems, among which we identified the integration and a posteriori error estimation of chaotic dynamical systems and the solution of Bayesian inverse problems, which are briefly presented here.

Chaotic differential equations

Let us consider the Lorenz system [17], which is defined by the following ODE

$$\begin{aligned} y_1' &= \sigma(y_2 - y_1), & y_1(0) &= -10, \\ y_2' &= y_1(\rho - y_3) - y_2, & y_2(0) &= -1, \\ y_3' &= y_1 y_2 - \beta y_3, & y_3(0) &= 40. \end{aligned} \tag{1}$$

It is well-known that for $\rho = 28$, $\sigma = 10$, $\beta = 8/3$, this equation has a chaotic behaviour, i.e., a small perturbation forces the trajectories to deviate from the true solution. Integrating numerically (1) the error which is introduced at each time step is indeed a perturbation, thus any numerical solution cannot be considered reliable. In order to explore the state space of this chaotic dynamical system, we introduce a random perturbation on the initial condition, implemented as a scalar Gaussian random variable $\varepsilon \sim \mathcal{N}(0, \sigma^2)$ and artificially added to the first component $x(t)$ at time $t = 0$. In Fig. 1 we show $M = 20$ numerical trajectories given by a second-order Runge–Kutta method for three different scales σ of the noise. It is possible to remark that in all the three cases, the numerical solutions almost coincide up to some time $\bar{t}$, thus diverging and showing the chaotic nature of the Lorenz system. It could be argued that up to time $\bar{t}$, the numerical solution offers a reliable approximation of the true solution as the dynamics have not yet switched to the chaotic regime. Nevertheless, it is unclear how to choose σ so that the amount of noise that is introduced is balanced with the numerical error. Probabilistic methods for differential equations such as the one presented in this work and the one introduced by Conrad et al. [6] provide a rigorous analysis that suggests how to introduce a source of artificial noise in a consistent manner.

A posteriori error estimator for ODEs

Building a rigorous and reliable a posteriori error estimator for the numerical solution of ODEs is still an issue for many classes of ODEs. Nonetheless, there exist many state of the art heuristic procedures to estimate the error and thus choose optimal time steps for integration. The common ground of these procedures is the choice of a tolerance value, that we denote by η, that should be realised in terms of the distance of the numerical solution from the true solution at final time. Apart from asymptotic analysis as the ones in [13, 15], where the limit $\eta \to 0$ is analysed, there is no theoretical guarantee that the error estimators are indeed a bound for the true error. However, for classes of stiff and non-stiff problems such heuristic estimators usually work very well [10, 11].

A classical approach is given by the so-called embedded methods, where numerical errors are estimated employing locally a higher order integrator. Let us consider again the Lorenz system (1) with the same initial condition and values of the parameters as above. We integrate it employing the embedded couple of explicit Euler and Heun methods, which are respectively a first and a second order method, to estimate the error at each time. In Fig. 2 we show that this traditional error estimator is not a reliable indicator of the true error, which is computed with respect to a reference solution obtained with a high-order Runge–Kutta method with a small time step.

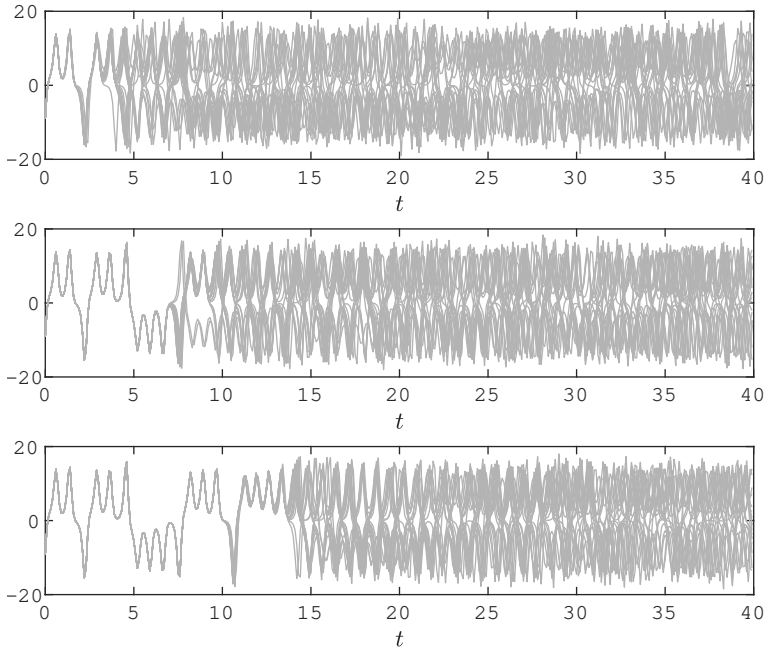

Figure 1: First component $x(t)$ of the solution of (1) with decreasing Gaussian perturbations on the initial condition from top to bottom.

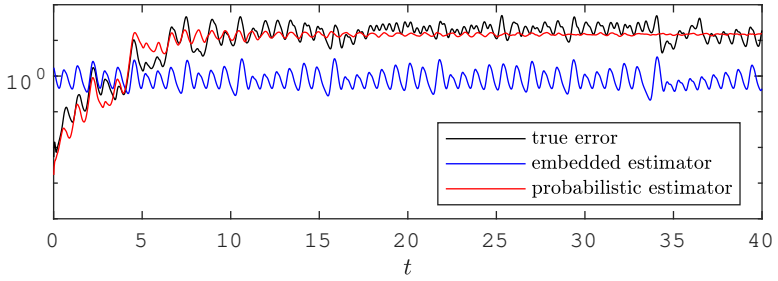

Figure 2: True error for the Lorenz system (black line), together with the error estimators given by the embedded couple explicit Euler – Heun (blue line) and by the standard deviation $\sigma(Y_n)$ of a probabilistic solution (red line).

A family of probabilistic solutions could give a consistent information on the numerical error. Let us denote by Y_n the solution given by the explicit Euler method perturbed in a probabilistic manner and by $\sigma_n = (\mathrm{tr}(\mathrm{Var}\, Y_n))^{1/2}$ its standard deviation, which is a candidate for the numerical error. We show in Fig. 2 that σ_n indeed follows qualitatively the true error in a more accurate way than the deterministic approach using embedded methods.

Bayesian inverse problems

The most employed example to justify the usefulness of probabilistic methods for differential equations is given by Bayesian inverse problems. The impact of a probabilistic component in the numerical approximation of inverse problems involving ODEs has already been presented in several works (e.g., [4–6]). In particular, the common underlying idea of these works is that if a deterministic integrator with a fixed finite time step is employed to approximate the solution of the ODE appearing in an inferential problem, the numerical error introduced by deterministic solvers can lead to inappropriate and non-predictive posterior concentrations. In the limit of an infinitely refined time discretisation the posterior distributions obtained with a classical numerical method will indeed tend to the true distribution, but for a fixed time step (i.e., for a fixed computational

budget) numerical error can lead to posterior concentrations away from the true value of the parameter of interest. These inappropriate solutions to inverse problems can be corrected employing a probabilistic integrator to solve the ODE, thus obtaining posterior distributions that reflect the uncertainty given by the numerical solver (see Fig. 4 for an example).

1.2 Contributions

The method we analyse in this paper is inspired from the work of Conrad et al. [6], where a probabilistic methods for ODEs is presented. This method consists in perturbing a deterministic numerical solution (e.g. arising from a Runge–Kutta discretisation) with an additive source of noise at each time step. Scaling opportunely the random term, they manage to obtain a probabilistic solution without altering the convergence of the underlying deterministic scheme.

An additive noise contribution could nonetheless produce disruptive effects on favourable geometric features of deterministic schemes. A direct example of this non-robust behaviour is given by ODEs for which the solution is supposed to stay positive and small. In this case, the addition of a random contribution could force the solution in the negative plane, hence the numerical solution could be physically meaningless. Chemical reactions with small population size for one species at some time of the evolution is a typical physical example of such a situation. An additive random term could force the solution on the negative plane with a non-zero probability, which can become significantly big in case the magnitude of one component is small. Other geometric properties of an underlying ODE are also destroyed when perturbing the flow by a noisy forcing term.

Motivated by these issues, we present in this work a new probabilistic method for ODEs based on a random selection of the time steps. Hence, the randomness of the scheme becomes intrinsic in contrast to the additive noise method. For this new robust probabilistic integrator, we are able to prove strong and weak convergence towards the exact solution of the underlying ODE. Precisely, setting the variance of the random time steps to be proportional to some power of a deterministic time step allows to retrieve the rates of the underlying Runge–Kutta integrator.

It has been pointed out by Kersting and Hennig [14] that probabilistic methods based on sampling should be equipped with a criterion to choose the number of samples, so that computational effort is not wasted or, conversely, the sample size is not insufficient to describe the dynamics in a probabilistic fashion. In order to address this issue, in this work we show that Monte Carlo estimators drawn from our probabilistic solver converge with respect to the time step in the mean square sense independently of the sample size. We are able to prove a similar property for the scheme proposed in [6].

A large variety of dynamical systems is characterised by geometrical properties of their flow map [9]. Most notably, Hamiltonian systems, which are employed for modelling a variety of physical phenomena, are endowed with the property of symplecticity. It is possible to obtain good approximations of the solutions of Hamiltonian systems via mimicking numerically the geometric properties of the exact flow, i.e., employing symplectic integrators. In particular, for symplectic integrators the energy function conserved by the exact flow is approximately conserved by numerical trajectories over long time spans, which in turn guarantees high-quality numerical solutions at the price of a rather low computational effort. While geometric properties of Runge–Kutta schemes have been analysed extensively in the deterministic case, they have not been considered yet for probabilistic numerical methods. The method we present in this work, being only an intrinsic modification of a Runge–Kutta integrator, is endowed with the geometric properties of its deterministic counterpart. In particular, we first show that our probabilistic scheme inherits the property of exact conservation of first integrals of the considered dynamics. Then, we show that in Hamiltonian systems the good approximation of the energy function given by symplectic schemes is preserved by our randomisation procedure over polynomially long times.

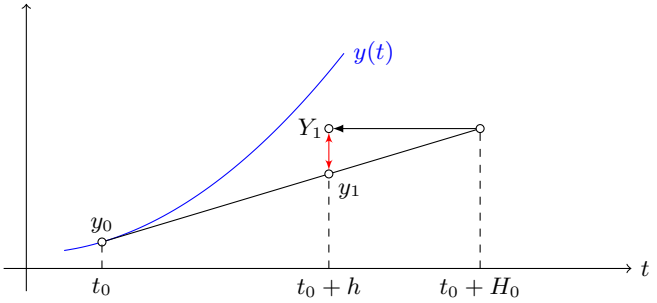

Figure 3: Graphical representation of one step of the RTS-RK method with $\Psi_h(y) = y + hf(y)$. The red arrow is the stochastic contribution due to random time-stepping.

1.3 Outline

The paper is organised as follows. In Section 2 we introduce the setting for probabilistic numerics and present our novel numerical scheme. We then show in Section 3 and Section 4 the properties of weak and mean square convergence of the numerical solution towards the exact solution of the ODE. In Section 5 we analyse the accuracy of Monte Carlo estimators drawn from the numerical solution. The geometric properties of the numerical scheme are presented in Section 6 and Section 7, while in Section 8 we introduce Bayesian inverse problems in the ODE setting, and show how our method can be integrated in existing sampling strategies. Finally, we show a variety of numerical experiments confirming our theoretical results in Section 9.

2 Random time step Runge–Kutta method

Let us consider a Lipschitz function $f\colon \mathbb{R}^d \to \mathbb{R}^d$ and the ODE

$$y' = f(y), \quad y(0) = y_0 \in \mathbb{R}^d. \tag{2}$$

In the following, we will write for simplicity the solution $y(t)$ of (2) in terms of the flow of the ODE. In particular, we consider the family $\{\varphi_t\}_{t\geq 0}$ of functions $\varphi_t\colon \mathbb{R}^d \to \mathbb{R}^d$ such that

$$y(t) = \varphi_t(y_0). \tag{3}$$

Given a time step h, let us consider a Runge–Kutta method which deterministically approximates the solution $\varphi_t(y_0)$ of (2). In particular, we can write the numerical solution y_k approximating $\varphi_{t_k}(y_0)$, with $t_k = kh$ in terms of the numerical flow $\{\Psi_t\}_{t\geq 0}$, with $\Psi_t\colon \mathbb{R}^d \to \mathbb{R}^d$, which is uniquely determined by the coefficients of the method, as

$$y_{k+1} = \Psi_h(y_k), \quad k = 0, 1, \dots. \tag{4}$$

In order to provide a probabilistic interpretation of the numerical solution rather than a series of point values, Conrad et al. propose the scheme defined by

$$Y_{k+1} = \Psi_h(Y_k) + \xi_k(h), \quad k = 0, 1, \dots, \tag{5}$$

where Y_k is a random variable approximating $y(t_k)$ with $Y_0 = y_0$, and $\xi_k(h)$ are opportunely scaled independent and identically distributed (i.i.d.) random variables with values in $\mathbb{R}^d$. Maintaining the same notation as in (5), in this work we propose a random time-stepping Runge–Kutta method (RTS-RK), i.e., the scheme defined defined by the recurrence relation

$$Y_{k+1} = \Psi_{H_k}(Y_k), \quad k = 0, 1, \dots, \tag{6}$$

where Y_k is still a random variable approximating $y(t_k)$ and the time steps H_k are locally given by a sequence of i.i.d. random variables with values in $\mathbb{R}^+$. A graphical representation of one step of the RTS-RK method is given in Fig. 3. Let us finally remark that the sequence Y_k, $k = 0, 1, \dots$, form a homogeneous Markov chain, as the transition probability is independent of the index k.

Remark 1. In terms of computational cost simulating the two methods (6) and (5) are almost equivalent, as they imply the same number of function evaluations as the underlying deterministic solver Ψ_h. Nonetheless, the random time-stepping method has the slight advantage that the random variable that has to be drawn at each time step takes values in $\mathbb{R}_+$, while for the additive noise ξ_k takes values in $\mathbb{R}^d$.

2.1 Assumptions and notation

We now present the main assumptions and notations which are used throughout the rest of this work. Firstly, we have to consider the possible values taken by the random step sizes, which have to satisfy restrictions that are necessary not to spoil the properties of deterministic methods.

Assumption 1. The i.i.d. random variables H_k satisfy for all $k = 0, 1, \dots$

(i) $H_k > 0$ a.s.,

(ii) there exists $h > 0$ such that $\mathbb{E}\, H_k = h$,

(iii) there exists $p \geq 1/2$ such that the scaled random variables $Z_k \coloneqq H_k - h$ satisfy

$$\mathbb{E}\, Z_k^2 = Ch^{2p+1}, \tag{7}$$

The class of random variable satisfying the hypotheses above is general. However, it is practical for an implementation point of view to have examples of these variables.

Example 1. Let us consider the random variables $\{H_k\}_{k\geq 0}$ such that

$$H_k \overset{\text{i.i.d.}}{\sim} \mathcal{U}(h - h^{p+1/2}, h + h^{p+1/2}), \quad 0 < h < 1, \quad p \geq 1/2. \tag{8}$$

We easily verify that the assumptions (i) and (ii) are verified as $h < 1$, and that (iii) is verified with $C = 1/3$. Another choice of random variables could simply be

$$H_k \overset{\text{i.i.d.}}{\sim} \log\mathcal{N}\big(\log h - \log\sqrt{1 + h^{2p}}, \log(1 + h^{2p})\big), \tag{9}$$

for which the properties above are trivially verified (with $C = 1$), provided $p > 1/2$.

We secondly introduce an assumption on the deterministic method underlying the RTS-RK scheme, identified by its numerical flow Ψ_h.

Assumption 2. The Runge–Kutta method defined by the numerical flow $\{\Psi_t\}_{t\geq 0}$ satisfies the following properties.

(i) For h small enough, there exists a constant $C > 0$ such that

$$\|\Psi_h(y) - \varphi_h(y)\| \leq Ch^{q+1}, \quad \forall y \in \mathbb{R}^d, \tag{10}$$

i.e., the deterministic solver has order q.

(ii) The map $t \mapsto \Psi_t(y)$ is of class $C^2(\mathbb{R}^+, \mathbb{R}^d)$ and Lipschitz continuous of constant L_Ψ, i.e.,

$$\|\Psi_t(y) - \Psi_s(y)\| \leq L_\Psi |t - s|, \quad \forall t, s > 0. \tag{11}$$

Remark 2. Depending on the domain of definition of the vector field f, the choice of an unbounded distribution for the time step could give rise to two critical issues. In particular,

(i) if $f\colon D \to \mathbb{R}^d$, where $D \in \mathbb{R}^d$ is a bounded open subset of $\mathbb{R}^d$, allowing the time step to assume unbounded values as, e.g., in case of the log-normal distribution (9), may force the solution outside D,

(ii) if Ψ_h is the numerical flow of an implicit method, the solution could be ill-posed.

In both the two cases above, we suggest to employ uniform time steps as in Example 1, which allow the time steps to be small enough almost surely. For the first issue, more sophisticated techniques of path rejection could be employed [19], but the mean-square convergence properties which will be examined in Section 4 would not hold.

In order to tackle the second issue presented in the Remark above, we introduce a further assumption.

Assumption 3. If the map Ψ_t is implicit, the time steps H_k satisfy $H_k \leq M < \infty$ almost surely, where M is small enough to allow the scheme to be well-posed.

Let us finally remark that the choice of the distribution of the time steps is artificial and therefore arbitrary. Hence, choosing a bounded distribution does not represent a limitation to the numerical scheme.

3 Weak convergence analysis

The first property of the RTS-RK method we wish to analyze is its weak convergence, which gives an indication about the behavior of the numerical solution (6) in the mean sense. Let us define the weak order of convergence.

Definition 1. The numerical method (6) has weak order r for (2) if for any function $\Phi \in \mathcal{C}^\infty(\mathbb{R}^d, \mathbb{R})$ with all derivatives bounded uniformly on $\mathbb{R}^d$ there exists a constant $C > 0$ independent of h such that

$$|\mathbb{E}\,\Phi(Y_k) - \Phi(y(kh))| \leq Ch^r, \tag{12}$$

for all $k = 1, 2, \ldots, N$ and $T = Nh$.

Let us introduce the Lie derivative of the flow $\mathcal{L} = f \cdot \nabla$, which allows us to adopt the semi-group notation for the exact solution of (2) and write for any smooth function Φ

$$\Phi(\varphi_h(y)) = e^{h\mathcal{L}}\Phi(y). \tag{13}$$

Moreover, let us remark that the probabilistic numerical solution $\{Y_k\}_{k\geq 0}$ forms a homogeneous Markov chain, and hence given $h > 0$ there exists an operator $\mathcal{P}_h$ such that

$$\mathbb{E}\left(\Phi(Y_{k+1}) \mid Y_k = y\right) = (\mathcal{P}_h\Phi)(y). \tag{14}$$

In order to have an analogy with the notation (13), we adopt the exponential form of the infinitesimal generator and denote in the following $\mathcal{P}_h = e^{h\mathcal{L}^h}$, where we explicitely write the dependence of the Markov generator on the step size h. Furthermore, thanks to the homogeneity of the Markov chain, we can write

$$\mathbb{E}\left(\Phi(Y_{k+1}) \mid Y_0 = y\right) = e^{h\mathcal{L}^h}\,\mathbb{E}\left(\Phi(Y_k) \mid Y_0 = y\right). \tag{15}$$

We can now state a result of local weak convergence of the probabilistic numerical solution.

Lemma 1 (Weak local order)**.** *Let Assumption 1, Assumption 3 and Assumption 2 hold. If* $\mathbb{E}\,|H_0^4| < \infty$*, there exists a constant* $C > 0$ *independent of* h *such that for any function* $\Phi \in \mathcal{C}^\infty(\mathbb{R}^d, \mathbb{R})$ *with all derivatives bounded uniformly on* $\mathbb{R}^d$

$$|\mathbb{E}(\Phi(Y_1) \mid Y_0 = y) - \Phi(\varphi_h(y))| \leq Ch^{\min\{2p+1, q+1\}}. \tag{16}$$

Proof. Let us expand the functional Φ computed on the numerical solution as

$$\begin{aligned}
\Phi(Y_1) &= \Phi(\Psi_{H_0}(Y_0)) \\
&= \Phi\Big(\Psi_h(Y_0) + (H_0 - h)\partial_t\Psi_h(Y_0) + \frac{1}{2}(H_0 - h)^2\partial_{tt}\Psi_h(Y_0) + \mathcal{O}(|H_0 - h|^3)\Big) \\
&= \Phi(\Psi_h(Y_0)) + \Big((H_0 - h)\partial_t\Psi_h(Y_0) + \frac{1}{2}(H_0 - h)^2\partial_{tt}\Psi_h(Y_0)\Big) \cdot \nabla\Phi(\Psi_h(Y_0)) \\
&\quad + \frac{1}{2}(H_0 - h)^2\partial_t\Psi_h(Y_0)\partial_t\Psi_h(Y_0)^\top : \nabla^2\Phi(\Psi_h(Y_0)) + \mathcal{O}(|H_0 - h|^3),
\end{aligned} \tag{17}$$

where we denote by $\nabla^2\Phi$ the Hessian matrix of Φ, and by : the inner product on matrices induced by the Frobenius norm on $\mathbb{R}^d$, i.e., $A : B = \mathrm{tr}(A^\top B)$. Taking the conditional expectation with respect to $Y_0 = y$ and applying Assumption 1 we get

$$\begin{aligned} e^{h\mathcal{L}^h}\Phi(y) - \Phi(\Psi_h(y)) = &\frac{1}{2}Ch^{2p+1}\partial_{tt}\Psi_h(y)\cdot\nabla\Phi(\Psi_h(y)) \\ &+ \frac{1}{2}Ch^{2p+1}\partial_t\Psi_h(y)\partial_t\Psi_h(y)^\top : \nabla^2\Phi(\Psi_h(y)) + \mathcal{O}(h^{3p+3/2}), \end{aligned} \tag{18}$$

where we exploited Hölder's inequality for the last term. Moreover, expanding Φ in y we get

$$\begin{aligned} \Phi(\Psi_h(y)) &= \Phi\left(\Psi_0(y) + h\partial_t\Psi_0(y) + \mathcal{O}(h^2)\right) \\ &= \Phi(y) + \mathcal{O}(h). \end{aligned} \tag{19}$$

which implies

$$\begin{aligned} e^{h\mathcal{L}^h}\Phi(y) - \Phi(\Psi_h(y)) = &\frac{1}{2}Ch^{2p+1}\partial_{tt}\Psi_h(y)\cdot\nabla\Phi(y) \\ &+ \frac{1}{2}Ch^{2p+1}\partial_t\Psi_h(y)\partial_t\Psi_h(y)^\top : \nabla^2\Phi(y) + \mathcal{O}(h^{2p+1}). \end{aligned} \tag{20}$$

Let us remark that thanks to Assumption 2.(i) we have

$$e^{h\mathcal{L}}\Phi(y) - \Phi(\Psi_h(y)) = \mathcal{O}(h^{q+1}). \tag{21}$$

Combining (21) and (20) we have the one-step weak error of the probabilistic method on the original ODE, i.e.,

$$e^{h\mathcal{L}}\Phi(y) - e^{h\mathcal{L}^h}\Phi(y) = \mathcal{O}(h^{\min\{2p+1,q+1\}}), \tag{22}$$

which proves the desired result. □

In order to obtain a result on the global order of convergence we need a further stability assumption, which is the same as Assumption 3 in [6].

Assumption 4. The function f is such that the operator $e^{h\mathcal{L}^h}$ satisfies for all functions $\Phi \in \mathbb{C}^\infty(\mathbb{R}^d, \mathbb{R})$ with all derivatives uniformly bounded in $\mathbb{R}^d$ and a positive constant L

$$\sup_{u\in\mathbb{R}^d} |e^{h\mathcal{L}^h}\Phi(u)| \leq (1 + Lh) \sup_{u\in\mathbb{R}^d} |\Phi(u)|. \tag{23}$$

Remark 3. Given the assumptions on f and Φ above, the exact solution satisfies

$$\sup_{u\in\mathbb{R}^d} |e^{h\mathcal{L}}\Phi(u)| \leq (1 + Lh) \sup_{u\in\mathbb{R}^d} |\Phi(u)|. \tag{24}$$

We can now state the main result on weak convergence.

Theorem 1 (Weak order)**.** *Let the assumptions of Lemma 1 and Assumption 4 hold. Then, there exists a constant $C > 0$ independent of h such that for all functions $\Phi \in \mathcal{C}^\infty(\mathbb{R}^d, \mathbb{R})$ with all derivatives bounded in $\mathbb{R}^d$*

$$|\mathbb{E}\,\Phi(Y_k) - \Phi(y(kh)))| \leq Ch^{\min\{2p,q\}}, \tag{25}$$

for all $k = 1, 2, \ldots, N$ and $T = Nh$.

Proof. Let us introduce the following notation

$$\begin{aligned} w_k(u) &= \Phi(\varphi_{t_k}(u)), \\ W_k(u) &= \mathbb{E}(\Phi(Y_k) \mid Y_0 = u). \end{aligned} \tag{26}$$

By the triangular inequality and the Markov property (15), we have

$$\begin{aligned} \sup_{u\in\mathbb{R}^d} |W_k(u) - w_k(u)| \leq &\sup_{u\in\mathbb{R}^d} |e^{h\mathcal{L}}w_{k-1}(u) - e^{h\mathcal{L}^h}w_{k-1}(u)| \\ &+ \sup_{u\in\mathbb{R}^d} |e^{h\mathcal{L}^h}w_{k-1}(u) - e^{h\mathcal{L}^h}W_{k-1}(u)|. \end{aligned} \tag{27}$$

We then apply Lemma 1 to the first term and Assumption 4 to the second, thus obtaining

$$\sup_{u\in\mathbb{R}^d}|W_k(u)-w_k(u)| \le Ch^{\min\{2p+1,q+1\}} + (1+Lh)\sup_{u\in\mathbb{R}^d}|w_{k-1}(u)-W_{k-1}(u)|. \tag{28}$$

Proceeding iteratively on the index k and noticing that $w_0 = W_0$, we obtain

$$\begin{aligned}\sup_{u\in\mathbb{R}^d}|w_k(u)-W_k(u)| &\le Ckh^{\min\{2p+1,q+1\}}\\ &\le CTh^{\min\{2p,q\}},\end{aligned} \tag{29}$$

which proves the result for any chosen initial condition y_0 in $\mathbb{R}^d$, as

$$|\mathbb{E}\,\Phi(Y_k)-\Phi(y(kh)))| \le \sup_{u\in\mathbb{R}^d}|W_k(u)-w_k(u)|. \tag{30}$$

□

Remark 4. In [6], Conrad et al. define ordinary and stochastic modified equations in order to prove a result of weak convergence applying techniques of backward error analysis. In particular, they show that their probabilistic solver approximates in the weak sense a stochastic differential equation (SDE) where the deterministic part is given by the original ODE. For our probabilistic solver, it is possible to prove that the numerical solutions approximates in the weak sense the solution of an SDE where the diffusion term depends on the derivative of the map $t \mapsto \Psi_t(y)$.

Remark 5. Let us recall that the random variable Y_k given by RTS-RK is thought as an approximation of $y(kh)$ regardless of the value of the sum of the random time steps. Hence, the comparison in (25) is legitimate and does not induce time misalignment between true and numerical solutions. This basic property applies to all results in the following.

4 Mean square convergence analysis

The second property of (6) we analyze is its mean square order of convergence, which gives an indication on the path-wise distance between each realisation of the numerical solution and the exact solution of (2). Let us define the mean square order of convergence.

Definition 2. The numerical method (6) has mean square order of convergence r for (2) if there exists a constant $C > 0$ independent of h such that

$$\left(\mathbb{E}\|Y_k - y(kh)\|^2\right)^{1/2} \le Ch^r \tag{31}$$

for all $k = 1, 2, \ldots, N$ and $T = Nh$.

Remark 6. Let us remark that the mean square convergence is stronger than the traditional strong convergence, since, by Jensen's inequality

$$\mathbb{E}\,\|Y_k - y(kh)\| \le \left(\mathbb{E}\|Y_k - y(kh)\|^2\right)^{1/2} \le Ch^r. \tag{32}$$

We start by analysing how the method converges with respect to the mean step size h in the local sense, i.e., after one step of the numerical integration.

Lemma 2 (Local mean square convergence)**.** *Under Assumption 1, Assumption 3 and Assumption 2 the numerical solution Y_1 given by one step of the RTS-RK method* (6) *satisfies*

$$\left(\mathbb{E}\|Y_1 - y(h)\|^2\right)^{1/2} \le Ch^{\min\{p+1/2,q+1\}}, \tag{33}$$

where C is a real positive constant independent of h and the coefficients p, q are given in the assumptions.

Proof. By triangular and Young's inequalities we have for all $y \in \mathbb{R}^d$

$$\mathbb{E}\|\Psi_{H_0}(y) - \varphi_h(y)\|^2 \leq 2\,\mathbb{E}\|\Psi_{H_0}(y) - \Psi_h(y)\|^2 + 2\|\Psi_h(y) - \varphi_h(y)\|^2. \tag{34}$$

We now consider Assumption 2 and Assumption 1, thus getting

$$\begin{aligned}\mathbb{E}\|\Psi_{H_0}(y) - \varphi_h(y)\|^2 &\leq 2L_\Psi^2\,\mathbb{E}|H_0 - h|^2 + 2C_1h^{2(q+1)} \\ &= 2L_\Psi^2 C_2 h^{2p+1} + 2C_1h^{2(q+1)} \\ &\leq C^2 h^{2\min\{p+1/2,q+1\}},\end{aligned} \tag{35}$$

which is the desired result with $C = \max\{2L_\Psi^2 C_2, 2C_1\}^{1/2}$. □

As a consequence of the one-step convergence, we can prove a result of global mean square convergence.

Theorem 2 (Global mean square convergence)**.** *Let f be globally Lipschitz and $t_k = kh$ for $k = 1, 2, \dots, N$, where $Nh = T$. Then, under the assumptions of Lemma 2 the numerical solution given by* (6) *satisfies*

$$\sup_{k=1,2,\dots,N} \left(\mathbb{E}\|Y_k - y(t_k)\|^2\right)^{1/2} \leq Ch^{\min\{p,q\}}, \tag{36}$$

where C is a real positive constant independent of h.

In order to prove this result, let us introduce the following lemmas.

Lemma 3. *Given the ODE* (2) *with f globally Lipschitz, then for any y and w in $\mathbb{R}^d$ and $h < 1$ we have*

$$\|\varphi_h(y) - \varphi_h(w)\| \leq (1 + Ch)\|y - w\|, \tag{37}$$

$$\|\varphi_h(y) - \varphi_h(w) - (y - w)\| \leq Ch\|y - w\|, \tag{38}$$

where C is a positive constant independent of h.

Lemma 4 (Lemma 1.6 of [18])**.** *Suppose that for arbitrary N and $k = 0, \dots, N$ we have*

$$u_k \leq (1 + Ah)u_{k-1} + Bh^r, \tag{39}$$

where $h = T/N$, $A > 0$, $B \geq 0$, $r \geq 1$ and $u_k \geq 0, k = 0, \dots, N$. Then

$$u_k \leq e^{AT}u_0 + \frac{B}{A}(e^{AT} - 1)h^{r-1}. \tag{40}$$

The proof of Lemma 3 follows from the definition of the flow and the Grönwall inequality, and the proof of Lemma 4 follows from the discrete Grönwall inequality. We can now prove the main result on mean square convergence.

Proof of Theorem 2. In the following, we denote by C a generic positive constant. Let us define $e_k^2 := \mathbb{E}\|Y_k - y(t_k)\|^2$. Adding and subtracting the exact flow applied to the numerical solution, we obtain

$$\begin{aligned}e_{k+1}^2 =& \mathbb{E}\|\Psi_{H_k}(Y_k) - \varphi_h(Y_k)\|^2 + \mathbb{E}\|\varphi_h(Y_k) - \varphi_h(y(t_k))\|^2 \\ &+ 2\,\mathbb{E}\left(\varphi_h(Y_k) - \varphi_h(y(t_k)), \Psi_{H_k}(Y_k) - \varphi_h(Y_k)\right),\end{aligned} \tag{41}$$

where we denote by $(\cdot, \cdot)$ the inner product in $\mathbb{R}^d$. Let us consider the three terms in (41) separately. For the first term, we have by Lemma 2

$$\mathbb{E}\|\Psi_{H_k}(Y_k) - \varphi_h(Y_k)\|^2 \leq Ch^{\min\{2p+1,2(q+1)\}}. \tag{42}$$

For the second term, since φ_h is Lipschitz with constant $(1 + Ch)$, we have

$$\mathbb{E}\|\varphi_h(Y_k) - \varphi_h(y(t_k))\|^2 \leq (1 + Ch)^2 e_k^2. \tag{43}$$

Let us now define $Z = \varphi_h(Y_k) - \varphi_h(y(t_k)) - (Y_k - y(t_k))$. Then we, can rewrite the inner product as

$$\begin{aligned}\mathbb{E}\left(\varphi_h(Y_k) - \varphi_h(y(t_k)), \Psi_{H_k}(Y_k) - \varphi_h(Y_k)\right) &= \mathbb{E}\left(Y_k - y(t_k), \Psi_{H_k}(Y_k) - \varphi_h(Y_k)\right) \\ &\quad + \mathbb{E}\left(Z, \Psi_{H_k}(Y_k) - \varphi_h(Y_k)\right).\end{aligned} \tag{44}$$

We bound the two terms in (44) separately. For the first term, by the law of total expectation, we have

$$\begin{aligned}\mathbb{E}\left(\big(Y_k - y(t_k)\big)^\top \big(\Psi_{H_k}(Y_k) - \varphi_h(Y_k)\big)\right) &= \mathbb{E}\,\mathbb{E}\left(\big(Y_k - y(t_k)\big)^\top \big(\Psi_{H_k}(Y_k) - \varphi_h(Y_k)\big) \mid Y_k\right) \\ &= \mathbb{E}\left(\big(Y_k - y(t_k)\big)^\top \mathbb{E}\left(\Psi_{H_k}(Y_k) - \varphi_h(Y_k) \mid Y_k\right)\right).\end{aligned} \tag{45}$$

Applying Cauchy–Schwarz inequality to the outer expectation we get

$$\begin{aligned}\mathbb{E}\left(\big(Y_k - y(t_k)\big)^\top \big(\Psi_{H_k}(Y_k) - \varphi_h(Y_k)\big)\right) &\le \left(\mathbb{E}\|\mathbb{E}\left(\Psi_{H_k}(Y_k) - \varphi_h(Y_k) \mid Y_k\right)\|^2\right)^{1/2} e_k \\ &\le C h^{\min\{2p+1, q+1\}} e_k,\end{aligned} \tag{46}$$

where we applied Lemma 1. We now consider the second term in (44). By the Cauchy–Schwarz inequality we have

$$\mathbb{E}\left(Z, \Psi_{H_k}(Y_k) - \varphi_h(Y_k)\right) \le \big(\mathbb{E}\|Z\|^2\big)^{1/2} \big(\mathbb{E}\|\Psi_{H_k}(Y_k) - \varphi_h(Y_k)\|^2\big)^{1/2}. \tag{47}$$

We now apply Lemma 3 and Lemma 2 to obtain

$$\mathbb{E}\left(Z, \Psi_{H_k}(Y_k) - \varphi_h(Y_k)\right) \le C h^{\min\{p+3/2, q+2\}} e_k. \tag{48}$$

We can hence bound the scalar product in (44) with Young's inequality and assuming $h < 1$ as

$$\begin{aligned}\mathbb{E}\left(\varphi_h(Y_k) - \varphi_h(y(t_k)), \Psi_{H_k}(Y_k) - \varphi_h(Y_k)\right) &\le C(h^{\min\{p+3/2, q+2\}}) e_k \\ &\le \frac{h e_k^2}{2} + C\frac{h^{\min\{2p+2, 2q+1\}}}{2}.\end{aligned} \tag{49}$$

Combining (42), (43) and (49), we have

$$e_{k+1}^2 \le C h^{\min\{2p+1, 2q+1\}} + (1 + Ch) e_k^2, \tag{50}$$

which implies the desired result by Lemma 4 and since $e_0 = 0$. □

Remark 7. Let us remark that the difference between global and local orders of convergence is not exactly one, as it usually is in the purely deterministic case. In fact, thanks to the independence of the random variables there is only a 1/2 loss in the random part of the exponent, while the natural loss of one order is verified in the deterministic component.

Remark 8. The result of mean square convergence suggests that a reasonable choice for the noise scale p is to fix $p = q$, where q is the order of the Runge–Kutta method Ψ_h. In this way, the properties of convergence of the underlying deterministic method are not spoiled, nonetheless getting a probabilistic interpretation of the numerical solution.

5 Monte Carlo estimators

The third property we analyze is the mean-square convergence of Monte Carlo estimators drawn from the random time-stepping Runge–Kutta method. Let us consider a function $\Phi \in \mathcal{C}^\infty(\mathbb{R}^d, \mathbb{R})$ with Lipschitz constant L_Φ and a final time $T > 0$. Moreover, let us introduce the notation

$Z = \Phi(y(T))$ and $Z_N = \Phi(Y_N)$. In general, the quantity Z_N is not accessible, and we have to replace it by its Monte Carlo estimator

$$\widehat{Z}_N = M^{-1}\sum_{i=1}^{M}\Phi(Y_N^{(i)}), \tag{51}$$

where $T = hN$ is the final time, M is the number of trajectories and we denote by $\{Y_N^{(i)}\}_{i=1}^{M}$ a set of i.i.d. realizations of the numerical solution. Hence, we are interested in studying the mean square error of the Monte Carlo estimator, which is defined as

$$\mathrm{MSE}(\widehat{Z}_N) = \mathbb{E}(Z - \widehat{Z}_N)^2. \tag{52}$$

In the following result, we prove that this quantity converges to zero independently of the number of trajectories M.

Theorem 3. *Under Assumption 1, Assumption 3 and Assumption 2, the Monte Carlo estimator $\widehat{Z}$ satisfies*

$$\mathrm{MSE}(\widehat{Z}_N) \leq C\Big(h^{2\min\{2p,q\}} + \frac{h^{2\min\{p,q\}}}{M}\Big), \tag{53}$$

where C is a positive constant independent of h and M.

Proof. Thanks to the classic decomposition of the MSE, we have

$$\mathrm{MSE}(\widehat{Z}_N) = \mathrm{Var}\,\widehat{Z}_N + \big(\mathbb{E}(\widehat{Z}_N - Z)\big)^2. \tag{54}$$

Applying Theorem 1 to the second term, we have

$$\mathrm{MSE}(\widehat{Z}_N) \leq \mathrm{Var}\,\widehat{Z}_N + Ch^{2\min\{2p,q\}}. \tag{55}$$

The variance of the estimator can be trivially bounded exploiting the Lipschitz continuity of Φ and the independence of the samples by

$$\mathrm{Var}\,\widehat{Z}_N \leq M^{-1}L_\Phi^2\,\mathbb{E}\|Y_N - y(T)\|^2. \tag{56}$$

Applying Theorem 2 we get

$$\mathrm{Var}\,\widehat{Z}_N \leq M^{-1}L_\Phi^2 Ch^{2\min\{p,q\}}, \tag{57}$$

which proves the desired result. □

Let us remark that with the choice $p = q$, which is the minimum p for which the order of convergence of the underlying deterministic method is not affected by the probabilistic setting, we have $\mathrm{MSE}(\widehat{Z}_N) \leq Ch^{2q}$ with $M = 1$. Hence, the Monte Carlo estimators drawn from (6) converge in the mean square sense independently of the number of samples M in (51). In the sub-optimal case $p < q$, one should carefully select the number of trajectories M so that the two terms in (53) are balanced.

6 Conservation of first integrals

Numerical methods for ODEs are often studied in terms of their geometric properties [9]. In particular, we investigate here whether the random choice of time steps in (6) spoils the properties of the underlying deterministic Runge–Kutta method. Let us recall the definition of first integral for an ODE.

Definition 3. Given a function $I\colon \mathbb{R}^d \to \mathbb{R}$, then $I(y)$ is a first integral of (2) if $I'(y)f(y) = 0$ for all $y \in \mathbb{R}^d$.

If this property of the ODE is conserved by a numerical integrator, i.e., if for the any $y \in \mathbb{R}^d$ it is true that $I(\Psi_h(y)) = I(y)$, then we say that the numerical method conserves the first integral. In particular, this implies that the invariant is conserved along the trajectory of the numerical solution, i.e., $I(y_k) = I(y_0)$ for all $k \geq 0$.

Example 2. To illustrate this concept we first discuss the case of linear first integrals, which can be seen as a general case of the conservation of mass in physical systems. Let us consider a linear first integral $I(y) = v^\top y$ and any Runge–Kutta method with coefficients $\{b_i\}_{i=1}^s$, $\{a_{ij}\}_{i,j=1}^s$. Then, we have for a time step $H_0 > 0$

$$I(Y_1) = v^\top y_0 + H_0 \textstyle\sum_{i=1}^s b_i v^\top f(y_0 + H_0 \sum_{j=1}^s a_{ij} K_j), \tag{58}$$

where $\{K_i\}_{i=1}^s$ are the internal stages of the Runge–Kutta method. Since $I(y)$ is a first integral, $v^\top f(y) = 0$ for any $y \in \mathbb{R}^d$. Hence $I(Y_1) = I(y_0)$ and iteratively $I(Y_k) = I(y_0)$ for all $k \geq 0$ along the numerical trajectory. The equality above shows that any RTS-RK method conserves linear first integrals path-wise, or in the strong sense.

It is known that no Runge–Kutta method can conserve any polynomial invariant of order $n \geq 3$ [9, Theorem IV.3.3]. Nonetheless, for some particular problems there exist tailored Runge–Kutta methods which can conserve polynomial invariants of higher order. We therefore can state the following general result.

Theorem 4. *If the Runge–Kutta scheme defined by Ψ_h conserves an invariant $I(y)$ for an ODE, then the numerical method* (6) *conserves $I(y)$ for the same ODE.*

Proof. If $I(\Psi_h(y)) = I(y)$ for any h, then $I(\Psi_{H_0}(y)) = I(y)$ for any value that H_0 can assume. □

We now consider quadratic first integrals, i.e., first integrals of the form $I(y) = y^\top C y$ with C a symmetric matrix, which are conserved by Runge–Kutta methods that satisfy the hypotheses of Cooper's theorem [9, Theorem IV.2.2]. The conservation of quadratic first invariants is of the utmost importance, e.g., for Hamiltonian systems, as it implies the symplecticity of the scheme. It is known [9, Theorem IV.2.1] that all Gauss methods conserve quadratic first integrals. The simplest member of this class of methods is the implicit midpoint rule, which is a one-stage method defined by coefficients $b_1 = 1$ and $a_{11} = 1/2$.

Corollary 1. *If the Runge–Kutta scheme defined by Ψ_h conserves quadratic first integrals then the numerical method* (6) *conserves quadratic first integrals.*

This result is a direct consequence of Theorem 4.

The properties above for the RTS-RK method are not satisfied by the additive noise method presented in [6]. In particular, let us remark that the conservation of first integrals is exact for any trajectory of the RTS-RK method, and is not an average property. In other words, we can say that (6) conserves linear first integrals in the strong sense. For the additive noise numerical method (5), we have

$$\begin{aligned} I(Y_1) &= v^\top y_0 + h \textstyle\sum_{i=1}^s b_i v^\top f(y_0 + h \sum_{j=1}^s a_{ij} K_j) + v^\top \xi_0(h), \\ &= v^\top (y_0 + \xi_0(h)). \end{aligned} \tag{59}$$

If the random variable ξ_0 is zero-mean, then $\mathbb{E}\, I(Y_1) = I(y_0)$ and iteratively along the solution $\mathbb{E}\, I(Y_k) = I(y_0)$. Linear first integrals are therefore conserved in average, but not in a path-wise fashion.

For quadratic first integrals, we have instead that the additive noise method does not conserve them neither path-wise nor in the weak sense, as we have

$$\begin{aligned} I(Y_1) &= (\Psi_h(y_0) + \xi_0(h))^\top S (\Psi_h(y_0) + \xi_0(h)) \\ &= I(y_0) + 2\xi_0(h)^\top S \Psi_h(y_0) + \xi_0(h)^\top S \xi_0(h). \end{aligned} \tag{60}$$

If the random variables are zero-mean and if there exists a matrix Q such that $\mathbb{E}\, \xi_0(h)\xi_0(h)^\top = Q h^{2p+1}$ for some $p \geq 1$ (Assumption 1 in [6]) we then have

$$\mathbb{E}\, I(Y_1) = I(y_0) + Q : S h^{2p+1}. \tag{61}$$

Hence, along the trajectories of the solution a bias is introduced in the first integral which persists even in the mean sense. In general, Theorem 4 is not valid for the additive noise method, as the random contribution drives the first integral far from its true value at each time step. This could produce in practice large deviations of the numerical approximation from the true solution, especially in the long time regime.

7 Hamiltonian systems

A class of dynamical systems of particular interest for their geometric properties are the Hamiltonian systems. Given a function $Q\colon \mathbb{R}^{2d} \to \mathbb{R}$, called the Hamiltonian, they can be written as

$$y' = J^{-1}\nabla Q(y), \quad y(0) = y_0 \in \mathbb{R}^{2d}, \tag{62}$$

where the matrix $J \in \mathbb{R}^{2d\times 2d}$ is defined as

$$J = \begin{pmatrix} 0 & I \\ -I & 0 \end{pmatrix}, \tag{63}$$

and where I is the identity matrix in $\mathbb{R}^{d\times d}$. The Hamiltonian Q is a first integral for (62), hence we require numerical integrators to conserve the energy, or at least not to deviate from its true value in an uncontrolled fashion. As it was shown in the previous section, when Q is a polynomial it is possible to obtain exact conservation with deterministic integrators and with their probabilistic counterparts obtained with the RTS-RK method. If Q is not a polynomial, exact conservation is in general not achievable, but a good approximation of the energy over long time spans is achievable through the notion of symplectic differentiable maps.

Definition 4 (Definition VI.2.2 in [9])**.** A differentiable map $g\colon U \to \mathbb{R}^{2d}$ (where $U \subset \mathbb{R}^{2d}$ is an open set) is called symplectic if the Jacobian matrix g' is everywhere symplectic, i.e., if

$$(g')^\top J g' = J. \tag{64}$$

It is well-known that the flow $\varphi_t\colon \mathbb{R}^{2d} \to \mathbb{R}^{2d}$ of any system of the form (62) is symplectic. In a natural manner, a numerical integrator is called symplectic if its numerical flow Ψ_h is a symplectic map. In the following, we will analyse both the local and global properties of the RTS-RK method built on symplectic integrators and applied to (62).

7.1 Symplecticity of the RTS-RK method

It has been pointed out [9,22] that applying an adaptive step size technique to a symplectic method can destroy its symplecticity. Therefore, Skeel and Gear [22] write any adaptive technique in function of a map $\tau(y,h)$ such that the k-th time step h_k is selected as $h_k = \tau(y_k, h)$, where h is a base value for the time step. Hence, in order to have again a symplectic method, the new condition to be satisfied is

$$V^\top J V = J, \quad V = \partial_y \Psi_{\tau(y,h)}(y) + \partial_t \Psi_{\tau(y,h)}(y)\partial_y \tau(y,h)^\top. \tag{65}$$

Let us now consider the RTS-RK method based on a symplectic deterministic integrator. We have the following lemma.

Lemma 5. *If the flow Ψ_h of the deterministic integrator is symplectic, then the flow of the random time-stepping probabilistic method* (6) *is symplectic.*

Proof. For the RTS-RK scheme, the k-th time step H_k is selected via a random mapping $\tau(y,h) = \tau(h) = h\Theta_k$, where Θ_k are opportunely scaled random variables such that H_k satisfies Assumption 1. Hence, τ is independent of y and with the notation introduced above

$$V = \partial_y \Psi_{\tau(h)}(y). \tag{66}$$

Therefore, by the symplecticity of Ψ_t the condition $V^\top JV = J$ is satisfied and the flow map of the RTS-RK method is symplectic. □

Let us remark that the local symplecticity of the flow map does not imply alone a good conservation of the Hamiltonian for the numerical solution. Global properties of approximation of the energy are therefore presented below.

7.2 Conservation of the Hamiltonian over long time

We now wish to study the mean conservation of the Hamiltonian along the trajectories of the RTS-RK method based on symplectic integrators. Our goal is obtaining a bound on the quantity $\mathbb{E}|Q(Y_n) - Q(y_0)|$ over long time. As stated above, showing theoretically long time conservation of the energy function in Hamiltonian systems requires backward error analysis. In the following, we will introduce the bases of this technique and show how they apply to our probabilistic integrator.

The first ingredient needed to perform a rigorous backward error analysis is a rather strong assumption on the regularity of the ODE.

Assumption 5 (see e.g. [9], Section IX.7). The function f is analytic in a neighbourhood of the initial condition y_0 and there exist constants $C, R > 0$ such that $\|f(y)\| \leq C$ for $\|y - y_0\| \leq 2R$.

In general, backward error analysis is based on determining a modified equation $y' = \widetilde{f}(y)$ such that the numerical approximation is its exact solution. Hence, the function $\widetilde{f}$ will both depend on the original ODE and on the numerical flow map Ψ_h. In particular, for an integrator of order q the modified equation is given by a function $\widetilde{f}$ defined as

$$\widetilde{f}(y) = f(y) + h^q f_{q+1}(y) + h^{q+1} f_{q+2}(y) + \dots, \tag{67}$$

where the functions $\{f_i\}_{i>q}$ are uniquely determined by f, its derivatives and by the coefficients of the Runge–Kutta method. The exactness of the numerical solution for the modified equation is nonetheless only formal, as the infinite sum defining $\widetilde{f}$ is not guaranteed to converge. Thus, it is necessary to truncate the sum in order to perform a rigorous analysis, i.e.,

$$\widetilde{f}(y) = f(y) + h^q f_{q+1}(y) + h^{q+1} f_{q+2}(y) + \dots + h^{N-1} f_N(y). \tag{68}$$

where $q < N < \infty$ is the truncation index. Let us remark that in the following we will always refer to the truncated function above when using the symbol $\widetilde{f}$. The truncation of the infinite sum implies that the numerical solution is not exact for the modified equation anymore. In particular, the error committed over one step on the modified equation is given by (see e.g. [9], Theorem IX.7.6)

$$\|\widetilde{\varphi}_h(y) - \Psi_h(y)\| \leq Che^{-\kappa/h}, \tag{69}$$

where κ and C are constants depending on the coefficients of the method and on the regularity of f.

It is possible to prove that for a Hamiltonian system (62) and a symplectic integrator the modified equation is still a Hamiltonian system, i.e., there exists a modified Hamiltonian $\widetilde{Q}$ defined as

$$\widetilde{Q}(y) = Q(y) + h^q Q_{q+1}(y) + \dots + h^{N-1} Q_N(y), \tag{70}$$

such that $\widetilde{f} = J^{-1}\nabla\widetilde{Q}$. The estimate (69) implies that the modified Hamiltonian is almost conserved by the symplectic integrator. In particular, if Q is Lipschitz, we have

$$|Q(\Psi_h(y)) - Q(y)| \leq Che^{-\kappa/h}. \tag{71}$$

The bound above guarantees that the modified Hamiltonian is well approximated for a long time, and as a consequence that the original Hamiltonian is almost conserved for the same time span. In particular, the following result is valid.

Theorem 5 (see e.g. [9], Theorem IX.8.1)**.** *Under Assumption 5 and for h sufficiently small, if the numerical solution y_n given by a symplectic method of order q applied to an Hamiltonian system is close enough to the initial condition y_0, then*

$$\begin{aligned} \widetilde{Q}(y_n) &= \widetilde{Q}(y_0) + \mathcal{O}(e^{-\kappa/2h}), \\ Q(y_n) &= Q(y_0) + \mathcal{O}(h^q). \end{aligned} \tag{72}$$

over exponentially long time intervals $nh \leq e^{\kappa/2h}$.

The randomisation of the time steps implies that a general modified equation does not exist. Nonetheless, thanks to Lemma 5, it is possible to construct locally a random Hamiltonian modified equation at each time step. We thus define at each step the random modified Hamiltonian as

$$\widehat{Q}_j(y) = Q(y) + H_j^q Q_{q+1}(y) + \ldots + H_j^{N-1} Q_N(y). \tag{73}$$

As for the deterministic case, the random modified Hamiltonian $\widehat{Q}$ will be almost conserved by the numerical flow. In particular, we can write

$$\widehat{Q}_j(\Psi_{H_j}(y)) = \widehat{Q}_j(y) + \eta_j, \tag{74}$$

for a random variable η_j such that $|\eta_j| \leq C H_j e^{-\kappa/H_j}$ almost surely. In order to prove the conservation of the Hamiltonian over long time for the RTS-RK method, it is necessary to introduce a technical assumption on the higher moments of the random time steps.

Assumption 6. There exists $\bar{r} > 1$ such that for any $1 < r < \bar{r}$, the random time steps $\{H_j\}_{j\geq 0}$ satisfy

$$\mathbb{E}\, H_j^r = h^r + C_r h^{2p+r-1}, \tag{75}$$

where p is defined in Assumption 1 and $C_r > 0$ satisfies $C_{2r} > 2C_r$ and is independent of h. Moreover, there exists $m, M > 0$ with $M > m$ such that $mh \leq H_j \leq Mh$ almost surely for all $j \geq 0$.

This assumption guarantees that the higher moments of the random time steps are close to the corresponding powers of h in the mean and mean square sense. In particular, it is possible to verify that

$$\begin{aligned} \mathbb{E}(H_j^r - h^r) &= C_r h^{2p+r-1}, \\ \mathbb{E}(H_j^r - h^r)^2 &= (C_{2r} - 2C_r) h^{2p+2r-1}. \end{aligned} \tag{76}$$

Moreover, for any $r, s > 1$ such that $r + s < R$, there exists $C > 0$ such that

$$\begin{aligned} \mathbb{E}(H_j^{r+s} - h^{r+s}) &= C h^s\, \mathbb{E}(H_j^r - h^r), \\ \mathbb{E}(H_j^{r+s} - h^{r+s})^2 &= C h^{2s}\, \mathbb{E}(H_j^r - h^r)^2. \end{aligned} \tag{77}$$

Finally, let us remark that Assumption 6 is satisfied for the uniform random time steps $H_j \overset{\text{i.i.d.}}{\sim} \mathcal{U}(h - h^{p+1/2}, h + h^{p+1/2})$ introduced in Example 1. Let us now prove a bound on the random variables η_j defined in (74).

Lemma 6. *Under Assumption 1, Assumption 3 and Assumption 6, the random variables η_j satisfy*

$$\mathbb{E}|\eta_j|^r \leq C h^{\min\{r, p+r-3/2\}} e^{-r\kappa/(Mh)}, \tag{78}$$

where $C > 0$ is independent of h and for all $r \in \mathbb{N}$ with $r \geq 1$.

The proof of this Lemma is given in the Appendix. It is now possible to prove a result of long conservation of the Hamiltonian for symplectic RTS-RK methods.

Theorem 6. *Under Assumption 3, Assumption 5, if Assumption 6 holds with $\bar{r}$ sufficiently large and Assumption 1 holds for $p \geq 3/2$, and if the numerical solution Y_n is close enough to the initial condition y_0 almost surely, there exist a constant $C > 0$ independent of h and n such that*

the solution given by the RTS-RK method built on a symplectic integrator of order q applied to a Hamiltonian system with Hamiltonian Q satisfies

$$\mathbb{E}|Q(Y_n) - Q(y_0)| \leq Ch^q, \tag{79}$$

for time intervals $t_n = nh$ of length

$$t_n = \mathcal{O}\big(\min\{h^{1-2p}, e^{\kappa/(4Mh)}h^{-(2p+2q-1)/4}, e^{\kappa/(2Mh)}\}\big) \tag{80}$$

where p is given in Assumption 1 and M in Assumption 6.

Proof. Let us first consider the modified Hamiltonian $\widetilde{Q}$ and expand the difference $\widetilde{Q}(Y_n) - \widetilde{Q}(y_0)$ in a telescopic sum as

$$\widetilde{Q}(Y_n) - \widetilde{Q}(y_0) = \sum_{j=0}^{n-1} \big(\widetilde{Q}(Y_{j+1}) - \widetilde{Q}(Y_j)\big). \tag{81}$$

We then consider each element of the sum, add and subtract the random modified Hamiltonian $\widehat{Q}_j$ computed in Y_{j+1} thus obtaining

$$\begin{aligned} \widetilde{Q}(Y_{j+1}) - \widetilde{Q}(Y_j) &= \widetilde{Q}(Y_{j+1}) - \widehat{Q}_j(Y_{j+1}) + \widehat{Q}_j(Y_{j+1}) - \widetilde{Q}(Y_j) \\ &= \widetilde{Q}(Y_{j+1}) - \widehat{Q}_j(Y_{j+1}) + \widehat{Q}_j(Y_j) - \widetilde{Q}(Y_j) + \eta_j. \end{aligned} \tag{82}$$

Hence, replacing the definition of $\widetilde{Q}$ and $\widehat{Q}_j$, we get

$$\widetilde{Q}(Y_{j+1}) - \widetilde{Q}(Y_j) = \sum_{k=q}^{N-1} (H_j^k - h^k)\big(Q_{k+1}(Y_j) - Q_{k+1}(Y_{j+1})\big) + \eta_j. \tag{83}$$

Going back to (81), introducing the notation $\Delta_{j,k} = Q_{k+1}(Y_j) - Q_{k+1}(Y_{j+1})$ and applying Jensen's inequality we obtain

$$\begin{aligned} \big(\mathbb{E}|\widetilde{Q}(Y_n) - \widetilde{Q}(y_0)|\big)^2 &= \Big(\mathbb{E}\Big|\sum_{j=0}^{n-1}\Big(\sum_{k=q}^{N-1}(H_j^k - h^k)\Delta_{j,k} + \eta_j\Big)\Big|\Big)^2 \\ &\leq \mathbb{E}\Big(\sum_{j=0}^{n-1}\Big(\sum_{k=q}^{N-1}(H_j^k - h^k)\Delta_{j,k} + \eta_j\Big)\Big)^2 \\ &= \sum_{j=0}^{n-1}\mathbb{E}\big((H_j^q - h^q)^2\Delta_{j,q}^2\big) \\ &\quad + 2\sum_{j=1}^{n-1}\sum_{i=0}^{j-1}\mathbb{E}\big((H_j^q - h^q)\Delta_{j,q}(H_i^q - h^q)\Delta_{i,q}\big) + R + S, \end{aligned} \tag{84}$$

where we decompose the remainder R in three terms $R = R_1 + R_2 + R_3$ defined as

$$\begin{aligned} R_1 &= \sum_{j=0}^{n-1}\sum_{k=q+1}^{N-1}\mathbb{E}\big((H_j^k - h^k)^2\Delta_{j,k}^2\big), \\ R_2 &= 2\sum_{j=0}^{n-1}\sum_{k=q+1}^{N-1}\sum_{l=q}^{k-1}\mathbb{E}\big((H_j^k - h^k)\Delta_{j,k}(H_j^l - h^l)\Delta_{j,l}\big), \\ R_3 &= \sum_{j=1}^{n-1}\sum_{i=0}^{j-1}\sum_{k=q+1}^{N-1}\sum_{l=2q-k+1}^{N-1}\mathbb{E}\big((H_j^k - h^k)\Delta_{j,k}(H_i^l - h^l)\Delta_{i,l}\big), \end{aligned} \tag{85}$$

and where the second remainder depends on the variables $\{\eta_j\}_{j\geq 0}$ and is given by $S = S_1 + S_2 + S_3 + S_4$, where

$$\begin{aligned}
S_1 &= \sum_{j=0}^{n-1} \mathbb{E}\,\eta_j^2, \\
S_2 &= 2\sum_{j=1}^{n-1}\sum_{i=0}^{j-1} \mathbb{E}\,\eta_j\,\mathbb{E}\,\eta_i, \\
S_3 &= 2\sum_{j=0}^{n-1}\sum_{k=q}^{N-1} \mathbb{E}\left(\eta_j(H_j^k - h^k)\Delta_{j,k}\right), \\
S_4 &= 2\sum_{j=1}^{n-1}\sum_{i=0}^{j-1}\Big(\mathbb{E}\,\eta_j \sum_{l=q}^{N-1}\mathbb{E}\left((H_i^l - h^l)\Delta_{i,l}\right) + \mathbb{E}\,\eta_i \sum_{k=q}^{N-1}\mathbb{E}\left((H_j^k - h^k)\Delta_{j,k}\right)\Big).
\end{aligned} \tag{86}$$

Under Assumption 5 we have $|\Delta_{j,k}| \leq CH_j$ for any $k = q, \ldots, N-1$, hence thanks to Assumption 6 it is possible to verify that there exist constants $C_i > 0$, $i = 1, 2, 3$ such that

$$\begin{aligned}
R_1 &\leq C_1 n h^{2(p+q+1)}, \\
R_2 &\leq C_2 n h^{2(p+q+1)}, \\
R_3 &\leq C_3 n^2 h^{2(2p+q+1)}.
\end{aligned} \tag{87}$$

Moreover, thanks to Lemma 6 there exist constants $\widehat{C}_i > 0$, $i = 1, 2, 3, 4$ such that

$$\begin{aligned}
S_1 &\leq \widehat{C}_1 h^{\min\{1,p-1/2\}} t_n e^{-2\kappa/(Mh)}, \\
S_2 &\leq \widehat{C}_2 h^{\min\{0,2p-3\}} t_n^2 e^{-2\kappa/(Mh)}, \\
S_3 &\leq \widehat{C}_3 h^{\min\{p+q+1/2,5p/4+q+1/8\}} t_n e^{-\kappa/(Mh)}, \\
S_4 &\leq \widehat{C}_4 h^{\min\{p+q-1/2,2p+q-2\}} t_n^2 e^{-\kappa/(Mh)},
\end{aligned} \tag{88}$$

where $t_n = nh$. Let us first consider the terms S_1 and S_2. Denoting $\widehat{S}_1 = S_1 + S_2$ and under the hypothesis $p \geq 3/2$, we have

$$\begin{aligned}
\widehat{S}_1^{1/2} &= \sqrt{S_1 + S_2} \\
&\leq C(\sqrt{ht_n} + t_n)e^{-\kappa/(Mh)} \\
&\leq C t_n e^{-\kappa/(Mh)}.
\end{aligned} \tag{89}$$

Let us now denote $\widehat{S}_2 = S_3 + S_4$. Under the hypothesis $p \geq 3/2$, we have

$$\begin{aligned}
\widehat{S}_2^{1/2} &= \sqrt{S_3 + S_4} \\
&\leq C(h^{(2p+2q+1)/4}\sqrt{t_n} + h^{(2p+2q-1)/4} t_n)e^{-\kappa/(2Mh)} \\
&\leq C h^{(2p+2q-1)/4} t_n e^{-\kappa/(2Mh)}.
\end{aligned} \tag{90}$$

Le us impose that $\widehat{S}_1^{1/2}$ and $\widehat{S}_2^{1/2}$ are exponentially bounded and hence negligible with respect to polynomial terms (see e.g. [9], Theorem IX.8.1) by fixing

$$t_n = \mathcal{O}(\min\{e^{\kappa/(4Mh)} h^{-(2p+2q-1)/4}, e^{\kappa/(2Mh)}\}), \tag{91}$$

so that

$$\begin{aligned}
\widehat{S}_1^{1/2} &= \mathcal{O}(e^{-\kappa/(2Mh)}), \\
\widehat{S}_2^{1/2} &= \mathcal{O}(e^{-\kappa/(4Mh)}).
\end{aligned} \tag{92}$$

Finally, replacing in (84) the expressions we obtained for the remainders, we get that the modified Hamiltonian admits the following bound

$$\begin{aligned}\mathbb{E}|\widetilde{Q}(Y_n) - \widetilde{Q}(y_0)| &\leq C\Big(\sum_{j=0}^{n-1} h^{2p+2q+1} + 2\sum_{j=1}^{n-1}\sum_{i=0}^{j-1} h^{4p+2q} + R + S\Big)^{1/2} \\ &\leq C\big(\sqrt{n}h^{p+q+1/2} + nh^{2p+q} + \sqrt{R} + \sqrt{S}\big) \\ &\leq C_1\sqrt{t_n}h^{p+q} + C_2 t_n h^{2p+q-1} + \mathcal{O}(e^{-\kappa/(4Mh)}),\end{aligned} \tag{93}$$

where the result holds for time spans of length given by (91). We now have thanks to the triangular inequality

$$\begin{aligned}\mathbb{E}|Q(Y_n) - Q(y_0)| &\leq \mathbb{E}|Q(Y_n) - \widetilde{Q}(Y_n)| + \mathbb{E}|Q(y_0) - \widetilde{Q}(y_0)| + \mathbb{E}|\widetilde{Q}(Y_n) - \widetilde{Q}(y_0)| \\ &\leq C_1\sqrt{t_n}h^{p+q} + C_2 t_n h^{2p+q-1} + C_4 h^q + \mathcal{O}(e^{-\kappa/(4Mh)}).\end{aligned} \tag{94}$$

Imposing $t_n = \mathcal{O}(h^{-2p+1})$ and combining this constraint with (91), we have that if t_n satisfies

$$t_n = \mathcal{O}\big(\min\{h^{1-2p}, e^{\kappa/(4Mh)}h^{-(2p+2q-1)/4}, e^{\kappa/(2Mh)}\}\big) \tag{95}$$

one gets

$$\mathbb{E}|Q(Y_n) - Q(y_0)| \leq Ch^q, \tag{96}$$

which is the desired result. □

Remark 9. The result of Theorem 6 is consistent with the theory of deterministic symplectic integrators. In fact, in the deterministic limit $p \to \infty$, the coefficient M in Assumption 6 tends to 1 and we have

$$\mathbb{E}|Q(Y_n) - Q(y_0)| = \mathcal{O}(h^q), \tag{97}$$

for exponentially long time spans $t_n = \mathcal{O}\big(e^{\kappa/(2h)}\big)$, which is consistent with the theory of deterministic symplectic integrators.

Remark 10. It has been observed (see for example [8,9]) that adopting variable step sizes in symplectic integration destroys the good properties of conservation of the Hamiltonian. In particular, the error on the Hamiltonian has a linear drift in time, i.e., the approximation has the same quality as the one given by a standard non-symplectic algorithm.

Remark 11. We introduce the assumption $p \geq 3/2$ in order to simplify the terms composing the remainder $\widehat{S}_1$. In case $1 \leq p < 3/2$, e.g. when the symplectic Euler method is employed ($q = 1$) and the natural scaling $p = q$ is chosen, the $\mathcal{O}(h^q)$ approximation of the Hamiltonian still holds but with a slight reduction in the exponential terms appearing in the time span of validity.

8 Bayesian inference inverse problems

It has been recently shown [4, 6, 16] that probabilistic methods for ordinary and partial differential equations guarantee robust results (with respect to the numerical discretisation error) in the context of Bayesian inverse problems. In this section, we briefly introduce a Bayesian inverse problem in the ODE setting and illustrate how the RTS-RK method can be employed in this framework.

Let us consider a function $f_\vartheta \colon \mathbb{R}^d \to \mathbb{R}^d$ which depends on a real parameter $\vartheta \in \Theta$, where Θ is an open subset of $\mathbb{R}^n$ and the ODE

$$y'_\vartheta = f_\vartheta(y), \quad y_\vartheta(0) = y_0 \in \mathbb{R}^d. \tag{98}$$

In order to simplify the notation, we consider y_0 to be a fixed initial condition. In general, y_0 could depend itself on ϑ. In the classical setting of numerical analysis, the main problem of interest is to determine the solution y_ϑ given the parameter ϑ. The inverse problem we consider is instead to determine ϑ through observations of the solution y_ϑ (or quantities derived from it). In the

Bayesian setting, the inverse problem is recast in terms of probability distributions, and the goal is to establish a probability measure on ϑ, the posterior measure, given observations and all the prior knowledge available.

Let us denote by $z \in \mathbb{R}^m$ the observable and by $\mathcal{G}\colon \Theta \to \mathbb{R}^m$ the forward operator, which can be written as $\mathcal{G} = \mathcal{O} \circ \mathcal{S}$, where $\mathcal{S}$ is the solution operator and $\mathcal{O}$ is the observation operator. In this case, $\mathcal{S}\colon \mathbb{R}^n \to \mathcal{C}([0,T])$ is the operator mapping ϑ into the solution y_ϑ, and $\mathcal{O}\colon \mathcal{C}([0,T]) \to \mathbb{R}^m$ maps the solution into the observable. Observations are then given by evaluations of the forward model corrupted by noise. In particular, we model noise as a Gaussian random variable $\varepsilon \sim \mathcal{N}(0, \Sigma_\varepsilon)$ independent of ϑ, so that observations read

$$z = \mathcal{G}(\vartheta) + \varepsilon. \tag{99}$$

Under these assumptions, the likelihood of the observations can be written as

$$\pi(z \mid \vartheta) = e^{-V_z(\vartheta)}, \tag{100}$$

where the function $V_z\colon \Theta \to \mathbb{R}$, called potential or negative log-likelihood, is given by

$$V_z(\vartheta) = \frac{1}{2}\big(\mathcal{G}(\vartheta) - z\big)^\top \Sigma_\varepsilon^{-1}\big(\mathcal{G}(\vartheta) - z\big). \tag{101}$$

The second building block of Bayesian inverse problems is the prior distribution, which we denote by $\pi_0(\vartheta)$. The prior encodes all the knowledge on the parameter that is known before observations are provided. In the following, we adopt a common abuse of notation, confounding measures and their probability density function.

Once the likelihood model and the prior distribution are established, it is possible to compute the posterior distribution $\pi(\vartheta \mid z)$ via Bayes' theorem, i.e.,

$$\pi(\vartheta \mid z) = \frac{\pi(z \mid \vartheta)\pi_0(\vartheta)}{\mathcal{Z}(z)}, \tag{102}$$

where $\mathcal{Z}(z)$ is the normalising constant given by

$$\mathcal{Z}(z) = \int_\Theta \pi(z \mid \vartheta)\pi_0(\vartheta)\,\mathrm{d}\vartheta. \tag{103}$$

Let us denote by $\mathcal{G}^h(\vartheta)$ the forward model where the solution operator is approximated by a Runge–Kutta method with time step h, and consequently with $V_z^h(\vartheta)$ and $\pi^h(z \mid \vartheta)$ the potential and the likelihood function obtained replacing $\mathcal{G}(\vartheta)$ with $\mathcal{G}^h(\vartheta)$. We can then define analogously the approximated posterior distribution $\pi^h(\vartheta \mid z)$ via Bayes' formula. In [24, Theorem 4.6], Stuart proves that the posterior distribution $\pi^h(\vartheta \mid z)$ converges to $\pi(\vartheta \mid z)$ with respect to h with the same rate as $V_z^h(\vartheta)$ converges to $V_z(\vartheta)$. Convergences is proved with respect to the Hellinger distance for a Gaussian prior, which is defined for probability density functions as

$$d_{\mathrm{Hell}}\big(\pi^h(\vartheta \mid z), \pi(\vartheta \mid z)\big)^2 = \frac{1}{2}\int_\Theta \left(\sqrt{\pi^h(\vartheta \mid z)} - \sqrt{\pi(\vartheta \mid z)}\right)^2 \mathrm{d}\vartheta. \tag{104}$$

Hence, when there is no restriction in computational resources and it is possible to choose h small, the approximated posterior distribution can be pushed arbitrarily close to the true posterior. The result is proved in [24] under the hypothesis of a Gaussian prior, but can be extended to a wider class of thin-tailed priors as done in [7] and to heavy-tailed priors as done in [25].

In this work we consider the case when h is fixed, and in particular we are interested in the case where the numerical error dominates the noise contribution. It has been shown via examples in [5,6] that in this small noise limit the approximated posterior distributions can be overly confident on the value of the parameter. In particular, the expectation of ϑ computed under the posterior distribution presents a bias with respect to the true value, which is not highlighted by the dispersion of the posterior itself. This undesirable phenomenon can be corrected employing a probabilistic

method, as the one presented by Conrad et al. in [6] or the RTS-RK method, to approximate the potential $V_z(\vartheta)$. Let us denote by $\xi \in \mathcal{X}$ the auxiliary random variable introduced by the probabilistic method. In the case of RTS-RK, we have $\xi = (H_0, H_1, \dots, H_{N-1})^\top$ and $\mathcal{X} \subset \mathbb{R}_+^N$. The likelihood function, denoted as $\pi^h_{\text{pr}}(z \mid \vartheta)$ is then approximated as

$$\pi^h_{\text{prob}}(z \mid \vartheta) = \mathbb{E}^\xi \, e^{-V_z^{h,\xi}(\vartheta)}. \tag{105}$$

where $V_z^{h,\xi}$ is the approximation of the potential function given by the probabilistic method. The corresponding posterior distribution π^h_{pr} is then obtained as

$$\pi^h_{\text{prob}}(\vartheta \mid z) = \frac{\pi^h_{\text{prob}}(z \mid \vartheta)\pi_0(\vartheta)}{\mathbb{E}^\xi \, \mathcal{Z}^{h,\xi}(z)}, \tag{106}$$

where the normalising constant is given by $\mathbb{E}^\xi \, \mathcal{Z}^{h,\xi}(z)$, where

$$\mathcal{Z}^{h,\xi}(z) = \int_\Theta e_z^{-V^{h,\xi}}(\vartheta)\pi_0(\vartheta)\mathrm{d}\vartheta. \tag{107}$$

Modifying the posterior in this manner allows to obtain qualitatively better results, which account for the uncertainty introduced by the numerical solver. Moreover, this posterior distribution still converges to the true posterior for $h \to 0$ as proved in [16], where (106) is called the marginal posterior.

In order to sample from the posteriors defined above we employ Markov chain Monte Carlo (MCMC) algorithms. In particular, thanks to the way the probabilistic posterior (106) is defined, the pseudo-marginal Metropolis Hastings (PMMH) algorithm [3] is a suitable choice for sampling. We note that in case of a deterministic approximation of the forward model, the standard random walk Metropolis Hastings is usually employed.

8.1 Analytical posteriors in a linear problem

In the limited case of linear problems and Gaussian prior it is possible to write explicitly the posterior distributions. Let us hence consider the following one dimensional ODE

$$y'(t) = -y(t), \quad y(0) = y_0. \tag{108}$$

Given $h > 0$, we consider the inferential problem of determining the true initial condition y_0^* from a single observation $d = \varphi_h(y_0^*) + \varepsilon$, where $\varphi_h(y_0^*) = y_0^* e^{-h}$ is the true solution at time $t = h$ and $\varepsilon \sim \mathcal{N}(0, \sigma^2)$ is a source of noise. If a Gaussian prior $\pi_0 = \mathcal{N}(0, 1)$ is given for y_0, the true posterior distribution is computable analytically and is given by

$$\pi(y_0 \mid d) = \mathcal{N}\Big(y_0; \frac{de^{-h}}{\sigma^2 + e^{-2h}}, \frac{\sigma^2}{\sigma^2 + e^{-2h}}\Big), \tag{109}$$

where $\mathcal{N}(x; \mu, \alpha^2)$ is the density of a Gaussian random variable of mean μ and variance α^2 evaluated in x. Consistently, if $\sigma^2 \to 0$, we have that $d \to y_0^* e^{-h}$ and therefore $\pi(y_0 \mid d) \to \delta_{y_0^*}$.

If we approximate $\varphi_h(y_0)$ for a given initial condition y_0 with a single step of the explicit Euler method (i.e., with step size h), we get $\Psi_h(y_0) = (1 - h)y_0$. Computing the posterior distribution obtained with this approximation leads to

$$\pi^h(y_0 \mid d) = \mathcal{N}\Big(y_0; \frac{(1-h)d}{\sigma^2 + (1-h)^2}, \frac{\sigma^2}{\sigma^2 + (1-h)^2}\Big). \tag{110}$$

In the limit of $\sigma^2 \to 0$, we get in this case that the posterior distribution tends to $\pi^h(y_0 \mid d) \to \delta_{\bar{y}}$, where $\bar{y} = e^{-h} y_0^*/(1 - h)$. The posterior distribution is hence tending to a biased Dirac delta with respect to the true value.

Let us consider the additive noise method (5) applied to the explicit Euler method, i.e., the random approximation $y(h) \approx Y_1$, where $Y_1 = (1-h)y_0 + \xi$ and where $\xi \sim \mathcal{N}(0, h^3)$, so that the method converges consistently with the deterministic method. In this case, the posterior distribution that we denote by $\pi^h_{\mathrm{pr,AN}}$ is given by

$$\pi^h_{\mathrm{pr,AN}}(y_0 \mid d) = \mathcal{N}\Big(y_0; \frac{(1-h)d}{\widetilde{\sigma}^2 + (1-h)^2}, \frac{\widetilde{\sigma}^2}{\widetilde{\sigma}^2 + (1-h)^2}\Big). \tag{111}$$

where $\widetilde{\sigma}^2 = \sigma^2 + h^3$. Hence, taking the limit $\sigma^2 \to 0$ gives

$$\pi^h_{\mathrm{pr,AN}}(y_0 \mid d) \to \mathcal{N}\Big(y_0; \frac{(1-h)e^{-h}y_0^*}{h^3 + (1-h)^2}, \frac{h^3}{h^3 + (1-h)^2}\Big), \tag{112}$$

which shows that while the asymptotic mean is still biased with respect to the true value, the uncertainty in the forward model is reflected by a positive variance. Let us now consider the random time step explicit Euler with step size distribution $H \sim \mathcal{U}(h - h^{p+1/2}, h + h^{p+1/2})$. In this case, the forward model is given by

$$Y_1 = y_0 - Hy_0 = (1-h)y_0 + Uy_0, \quad U \sim \mathcal{U}(-h^{p+1/2}, h^{p+1/2}). \tag{113}$$

Hence, disregarding all multiplicative constants that are independent of y_0 and setting $p = q = 1$, we get the posterior

$$\pi^h_{\mathrm{pr,RTS}}(y_0 \mid d) \propto \exp\Big(-\frac{y_0^2}{2}\Big)\frac{1}{y_0}\Big(\Phi\Big(\frac{((1-h)+h^{3/2})y_0 - d}{\sigma}\Big) - \Phi\Big(\frac{((1-h)-h^{3/2})y_0 - d}{\sigma}\Big)\Big), \tag{114}$$

where Φ denotes the cumulative distribution function of a standard Gaussian random variable. Since we require in Assumption 1.(i) that $H > 0$ almost surely, the time step H cannot be Gaussian and the closed-form expression of the posterior is not as neatly defined as in the additive noise case. In the limit for $\sigma \to 0$, we get the limiting distribution

$$\pi^h_{\mathrm{pr,RTS}}(y_0 \mid d) \propto \exp\Big(-\frac{y_0^2}{2}\Big)\frac{1}{y_0}\chi_{\{y_{\min} \le y_0 \le y_{\max}\}}, \tag{115}$$

where $y_{\min}$ and $y_{\max}$ are given by

$$y_{\min} = \frac{e^{-h}y_0^*}{((1-h)+h^{3/2})}, \quad y_{\max} = \frac{e^{-h}y_0^*}{((1-h)-h^{3/2})}. \tag{116}$$

It is hence possible to remark that for the RTS-RK method the variance of the posterior distribution is not collapsing to zero for $\sigma \to 0$ as in the deterministic case.

We fix $h = 0.5$ and consider $\sigma = \{0.1, 0.05, 0.025, 0.0125\}$, thus generating four observational noises η_i as $\eta_i = \sigma_i Z$ for a random variable $Z \sim \mathcal{N}(0,1)$. In Fig. 4 we show the posteriors (109), (110), (112) and (114), which confirm our claim, i.e., that probabilistic methods take into account the variability in the forward model caused by the numerical approximation and transfer it to the posterior belief.

9 Numerical experiments

In this section, we present a series of numerical experiments that illustrate the versatility and usefulness of our new random time stepping method. These experiments also corroborate the theoretical results presented in the previous sections.

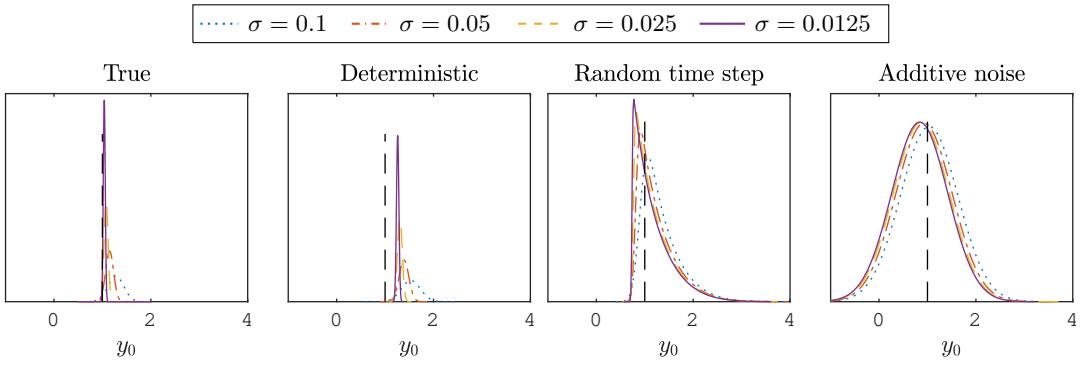

Figure 4: Analytical posterior distributions in the linear case of Section 8.1 for the true solution and its approximations with the deterministic explicit Euler method and the two probabilistic versions with additive noise (5) and with random time steps (6). In this case, $h = 0.5$ and the variance σ^2 of the observation error is reduced progressively. The true value of the initial condition $y_0^* = 1$ is shown with a vertical black dashed line.

Method	ET					RK4				
q	2					4				
p	0.5	1	1.5	2	2.5	2.5	3	3.5	4	4.5
$\min\{p, q\}$	0.5	1	1.5	2	2	2.5	3	3.5	4	4
strong order	0.51	1.02	1.54	2.01	2.01	2.50	3.01	3.56	4.02	4.01

Table 1: Mean square order of convergence for the random time-stepping explicit trapezoidal (ET) and fourth-order Runge–Kutta (RK4) as a function of the value of p of Assumption 1.

9.1 Mean square order of convergence

In order to verify the result predicted in Theorem 2, we consider the FitzHug–Nagumo equation, which is defined as

$$\begin{aligned} y_1' &= c\big(y_1 - \frac{y_1^3}{3} + y_2\big), \qquad y_1(0) = -1, \\ y_2' &= -\frac{1}{c}(y_1 - a + by_2), \quad y_2(0) = 1, \end{aligned} \tag{117}$$

where a, b, c are real parameters with values $a = 0.2$, $b = 0.2$, $c = 3$. We integrate the equation from time $t_0 = 0$ to final time $T = 1$. The reference solution is generated with an high order method on a fine time scale. We consider as deterministic solvers the explicit trapezoidal rule and the classic fourth order Runge–Kutta method, which verify Assumption 2 with $q = 2$ and $q = 4$ respectively. Moreover, we consider uniform random time steps as in Example 1, where we vary p in order to verify the order of convergence predicted in Theorem 2. We vary the mean time step h taken by the random time steps H_n in the range $h_i = 0.01 \cdot 2^{-i}$, with $i = 0, 1, \ldots, 4$. Then, we simulate 10^3 realizations of the numerical solution Y_{N_i}, with $N_i = T/h_i$ for $i = 0, 1, \ldots, 4$, and compute the approximate mean square order of convergence for each value of h with a Monte Carlo mean. Results (Table 1) show that the orders predicted theoretically by Theorem 2 are confirmed numerically.

9.2 Weak order of convergence

We now verify the weak order of convergence predicted in Theorem 1. For this experiment we consider the ODE (117) as well, with the same time scale and parameters as above. The reference solution at final time is generated in this case as well with an high-order method on a fine time scale. The deterministic integrators we choose in this experiment are the explicit trapezoidal rule

Method	ET			RK4				
q	2			4				
p	1	1.5	2	1	1.5	2	3	4
$\min\{2p, q\}$	1	2	2	1	2	3	4	4
weak order	0.98	2.06	2.12	0.90	1.96	3.01	3.97	4.08

Table 2: Weak order of convergence for the random time-stepping explicit trapezoidal (ET) and fourth-order Runge–Kutta (RK4) as a function of the value of p of Assumption 1.

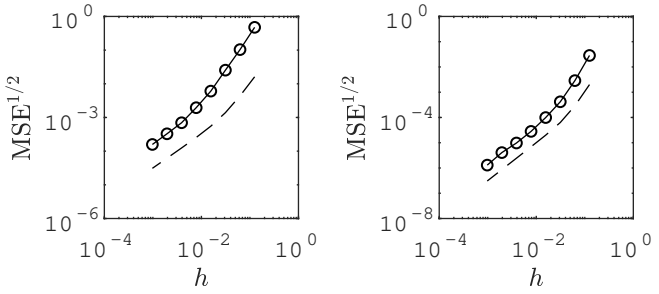

Figure 5: Convergence of the MSE of the Monte Carlo estimator for the random time-stepping explicit trapezoidal (ET) (left figure) and fourth-order Runge–Kutta (RK4) (right figure). The dashed line corresponds to the order predicted in Theorem 3 with $M = 10^3$ for ET and $M = 10^4$ for RK4.

and the classic fourth-order Runge–Kutta method. The random steps are uniform as in Example 1. We vary their mean in the range $h_i = 0.1 \cdot 2^{-i}$ with $i = 0, 1, \ldots, 5$, and we vary the value of p in Assumption 1 in order to verify the theoretical result of Theorem 1. The function $\Phi\colon \mathbb{R}^d \to \mathbb{R}$ of the solution we consider is defined as $\varphi(x) = x^\top x$. Finally, we consider 10^6 trajectories of the numerical solution in order to approximate the expectation with a Monte Carlo sum. Results (Table 2) show that the order of convergence predicted theoretically is confirmed by numerical experiments.

9.3 Monte Carlo estimator

We shall now verify numerically the validity of Theorem 3. We consider the ODE (117), with final time $T = 1$ and the same parameters as above. In this case as well, we consider the explicit trapezoidal rule and the fourth-order explicit Runge–Kutta method with uniform random time steps having mean $h_i = 0.125 \cdot 2^{-i}$ with $i = 0, 1, \ldots, 7$. For the explicit trapezoidal rule, we fix $M = 10^3$ and $p = 1$, so that for bigger values of h the first term in the bound presented in Theorem 3 dominates, while in the regime of small h, the higher order of the first term makes the second term larger in magnitude. This behaviour results in the change of slope in the convergence plot which can be observed in Fig. 5, both in the theoretical estimate and in the numerical results. We perform the same experiment using the fourth-order explicit Runge–Kutta method, fixing $M = 10^4$ and $p = 1.5$, thus obtaining a numerical confirmation of the theoretical result.

9.4 Robustness

In this numerical experiment we verify the robustness of RTS-RK when applied to chemical reactions. Let us consider the Peroxide-Oxide chemical reaction, which is macroscopically defined by the following balance equation

$$\mathrm{O_2} + 2\mathrm{NADH} + 2\mathrm{H^+} \to 2\mathrm{H_2O} + 2\mathrm{NAD^+}, \tag{118}$$

where NADH and $\mathrm{NAD^+}$ are the oxidized and reduced form of the nicotinamide adenine dinucleotide (NAD) respectively. This reaction has to be catalyzed by an enzyme to take place, which reacts with

the reagents to create intermediate products of the reaction. A successful model [20] to describe the time-evolution of the chemical system is the following

$$\begin{aligned} &\mathrm{B}+\mathrm{X} \xrightarrow{k_1} 2\mathrm{X}, \quad 2\mathrm{X} \xrightarrow{k_2} 2\mathrm{Y}, \quad \mathrm{A}+\mathrm{B}+\mathrm{Y} \xrightarrow{k_3} 3\mathrm{X}, \\ &\mathrm{X} \xrightarrow{k_4} \mathrm{P}, \quad \mathrm{Y} \xrightarrow{k_5} \mathrm{Q}, \quad \mathrm{X}_0 \xrightarrow{k_6} \mathrm{X}, \\ &\mathrm{A}_0 \xleftrightarrow{k_7} \mathrm{A}, \quad \mathrm{B}_0 \xrightarrow{k_8} \mathrm{B}. \end{aligned} \tag{119}$$

Here, A and B are respectively $[O_2]$ and [NADH], P, Q are the products and X, Y are intermediates results of the reaction process. It is therefore possible to model the time evolution of the reaction with the following system of nonlinear ODEs

$$\begin{aligned} \mathrm{A}' &= k_7(\mathrm{A}_0-\mathrm{A})-k_3\mathrm{ABY}, & \mathrm{A}(0)&=6, \\ \mathrm{B}' &= k_8\mathrm{B}_0-k_1\mathrm{BX}-k_3\mathrm{ABY}, & \mathrm{B}(0)&=58, \\ \mathrm{X}' &= k_1\mathrm{BX}-2k_2\mathrm{X}^2+3k_3\mathrm{ABY}-k_4\mathrm{X}+k_6\mathrm{X}_0, & \mathrm{X}(0)&=0, \\ \mathrm{Y}' &= 2k_2\mathrm{X}^2-k_5\mathrm{Y}-k_3\mathrm{ABY}, & Y(0)&=0, \end{aligned} \tag{120}$$

where $\mathrm{A}_0=8$, $\mathrm{B}_0=1$, $\mathrm{X}_0=1$ and the real parameters k_i, $i=1,\dots,8$ representing the reaction rates take values

$$\begin{aligned} &k_1=0.35, \quad k_2=250, \quad k_3=0.035, \quad k_4=20, \\ &k_5=5.35, \quad k_6=10^{-5}, \quad k_7=0.1, \quad k_8=0.825. \end{aligned} \tag{121}$$

It has been shown [20] that for these values of the parameters the system exhibits a chaotic behavior. In particular, at long time the trajectories are captured in a strange attractor, and the system shows a strong sensitivity to perturbations on the initial condition.

Since the components of the solution represent the concentration of chemicals, we require the numerical solution to be positive. Apart from physical considerations, numerically we observe that if one of the components takes negative values, the solution shows strong instabilities. For the RTS-RK method, the distribution of the random time steps can be selected (see for example Example 1) so that the probability of obtaining a negative solution is zero. In contrast, for the additive noise method we can have disruptive effects even for h small if the solution has a small magnitude, as the probability for negative populations will never be zero. Hence, in this case employing the additive noise method likely produces instabilities regardless of the chosen time step.

Let us apply the additive noise method (5) and the random time-stepping scheme (6) to equation (120). We choose $h=0.05$ as the mean of uniformly distributed time steps for (6) and as the time step for (5), while we employ the Runge–Kutta–Chebyshev method (RKC) [26] as deterministic integrator. As the problem is stiff, stabilised methods prevent a step size restriction while remaining explicit. We note that the RKC method is a stabilized numerical integrator of first order and that higher order explicit stabilized methods such as ROCK2 or ROCK4 [1, 2] could also be used as deterministic solvers for the RTS-RK method. It can be seen in Fig. 6 that the RTS-RK method conserves the positivity of the numerical solution while capturing the chaotic nature of the chemical reaction. In contrast, the additive noise scheme produces negative values, thus showing strong instabilities in the long-time behavior. In particular, all the numerical trajectories turn negative or diverge before approximately $t=25$, which is the reason why after this time they are not displayed in Fig. 6.

9.5 Conservation of quadratic first integrals

A simple model for the two-body problem in celestial mechanics is the Kepler system with a perturbation, which reads

$$\begin{aligned} w_1' &= v_1, \quad v_1' = -\frac{w_1}{\|q\|^3}-\frac{\delta w_1}{\|q\|^5}, \\ w_2' &= v_2, \quad v_2' = -\frac{w_2}{\|q\|^3}-\frac{\delta w_2}{\|q\|^5}, \end{aligned} \tag{122}$$

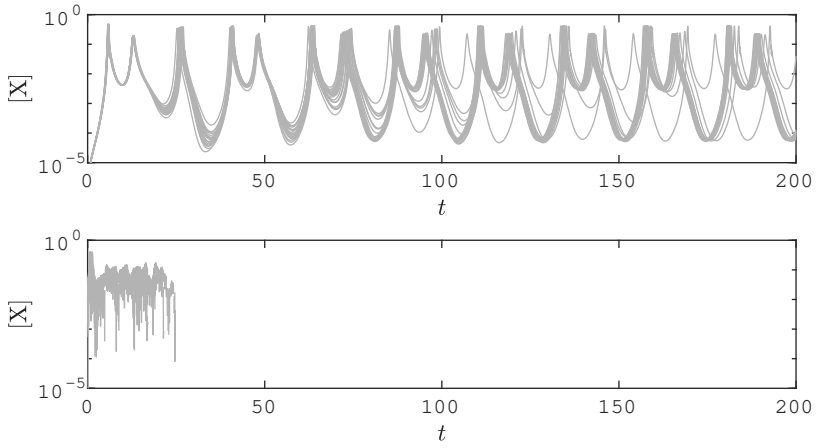

Figure 6: Fifty trajectories of the numerical value of the concentration of the X species for the random time-stepping and additive noise methods (above and below respectively).

where v_1, v_2 are the two components of the velocity and w_1, w_2 are the two components of the position. We assume the perturbation parameter δ to be equal to 0.015 and the initial condition to be

$$w_1(0) = 1 - e, \quad w_2(0) = 0, \quad v_1(0) = 0, \quad v_2(0) = \sqrt{(1+e)/(1-e)}, \tag{123}$$

where $e = 0.6$ is the eccentricity. It is well-known that this equation has the Hamiltonian and the angular momentum as quadratic first integrals. In particular, we focus here on the angular momentum, which reads

$$I(v, w) = w_1 v_2 - w_2 v_1. \tag{124}$$

We consider the simplest Gauss collocation method, namely the implicit midpoint rule, as the deterministic Runge–Kutta method. It is known that Gauss collocation methods conserve quadratic first integrals. According to Theorem 4, we expect therefore that the random time-stepping method (6) implemented with Ψ_h given by the implicit midpoint rule conserves also quadratic first integrals. We therefore integrate (122) with uniformly distributed mean time step $h = 0.01$ from time $t = 0$ to time $t = 4000$ which corresponds to approximately 636 revolutions of the system (long-time behavior). Moreover, we consider the additive noise method (5) with $h = 0.01$, expecting that the first integral will not be conserved. We observe in Fig. 7 that the method (6) conserves the angular momentum, while for the method (5) the approximate conservation of the quadratic first integral shown in (61) is lost when integrating (122) over long time.

9.6 Hamiltonian systems

Let us consider the pendulum problem, which is given by the Hamiltonian $Q\colon \mathbb{R}^2 \to \mathbb{R}$ defined by

$$Q(v, w) = \frac{v^2}{2} - \cos w, \tag{125}$$

where $y = (v, w)^\top \in \mathbb{R}^2$. We wish to study the validity of Theorem 6, i.e., show that the mean error on the Hamiltonian is of order $\mathcal{O}(h^q)$ for time spans of polynomial length and then it grows proportionally to the square root of time. We consider the initial condition $(v_0, w_0) = (1.5, -\pi)$ and integrate the equation employing RTS-RK based on the implicit midpoint method ($q = 2$) choosing $p = q$, which is the optimal scaling of the noise. We choose uniform time steps, vary their mean $h \in \{0.2, 0.1, 0.05, 0.025\}$, integrate the dynamical system up to the final time $T = 10^6$ and study the time evolution of the mean numerical error on the Hamiltonian Q. Results are shown in Fig. 8, where it is possible to notice that the error is bounded by $\mathcal{O}(h^q)$ (horizontal black lines) for long time spans. After this stationary phase, the error on the Hamiltonian appears to grow as the

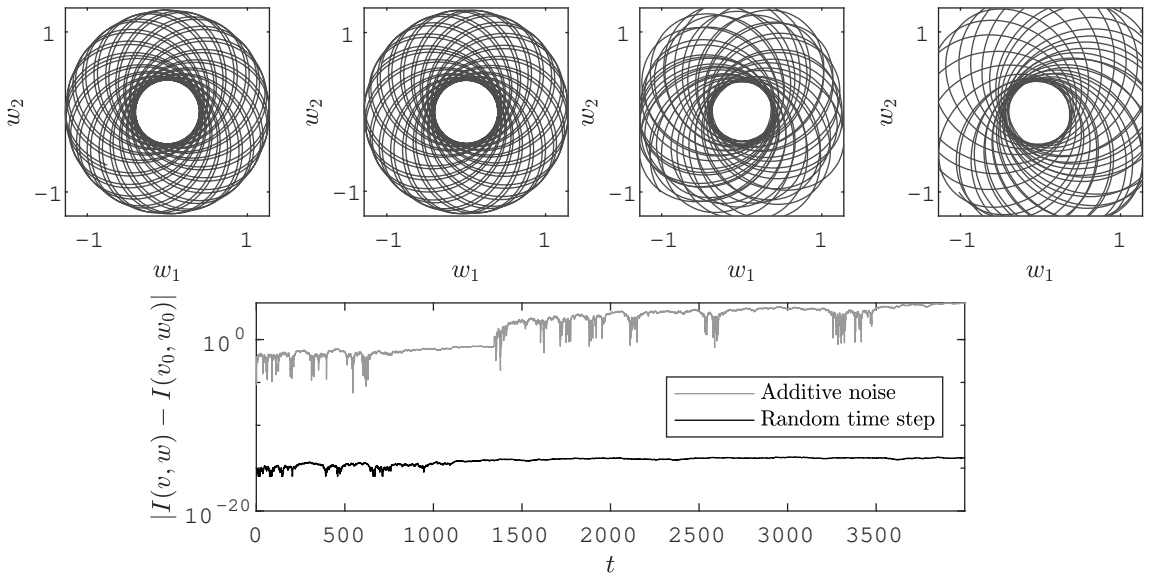

Figure 7: Trajectories of (122) given by the RTS-RK method (6) for $0 \leq t \leq 200$ and $3800 \leq t \leq 4000$ (first and second figures), and by the additive noise method (5) for $0 \leq t \leq 200$ and $200 \leq t \leq 400$ (third and fourth figures). Error on the angular momentum for $0 \leq t \leq 4000$ given by the two methods.

square root of time. The oscillations of the error which are shown in Fig. 8 are present even when integrating the pendulum system with a deterministic symplectic scheme.

9.7 Bayesian inferential problems

For the last numerical experiment we consider the Hénon–Heiles equation, a Hamiltonian system with energy $Q\colon \mathbb{R}^4 \to \mathbb{R}$ defined by

$$Q(v,w) = \frac{1}{2}\|v\|^2 + \frac{1}{2}\|w\|^2 + w_1^2 w_2 - \frac{1}{3}w_2^3, \tag{126}$$

where $v, w \in \mathbb{R}^2$ are the velocity and position respectively and where we denote by $y = (v,w)^\top \in \mathbb{R}^4$ the solution. We consider an initial condition such that $Q(y_0) = 0.13$, for which the system presents a chaotic behaviour [12]. In the spirit of Section 8, we are interested in recovering the true value of the initial condition y_0 through a single observations y_{obs} of the solution (v,w) at a fixed time $t_{\text{obs}} = 10$. The exact forward operator $\mathcal{G}$ is therefore defined as $\mathcal{G}(y_0) = \varphi_{t_{\text{obs}}}(y_0)$. Noise is then assumed to be a Gaussian random variable $\varepsilon \sim \mathcal{N}(0, \sigma_\varepsilon^2 I)$, where $\sigma_\varepsilon = 5 \cdot 10^{-4}$, and we fix a standard Gaussian prior on the initial condition, i.e., $\pi_0 = \mathcal{N}(0, I)$.

Since the equation is Hamiltonian, we choose to employ a classical second-order ($q = 2$) symplectic method, the Störmer–Verlet scheme [9, 23, 27], for which one step is defined in the general case as

$$\begin{aligned} v_{n+1/2} &= v_n - \frac{h}{2}\nabla_w Q(v_n, w_n), \\ w_{n+1} &= w_n + \frac{h}{2}\big(\nabla_v Q(v_{n+1/2}, w_n) + \nabla_v Q(v_{n+1/2}, w_{n+1})\big), \\ v_{n+1} &= v_{n+1/2} - \frac{h}{2}\nabla_w Q(v_{n+1/2}, w_{n+1}). \end{aligned} \tag{127}$$

As the Hamiltonian Q given by (126) is separable, i.e., $Q(v,w) = Q_1(v) + Q_2(w)$, where $Q_1, Q_2\colon \mathbb{R}^2 \to$

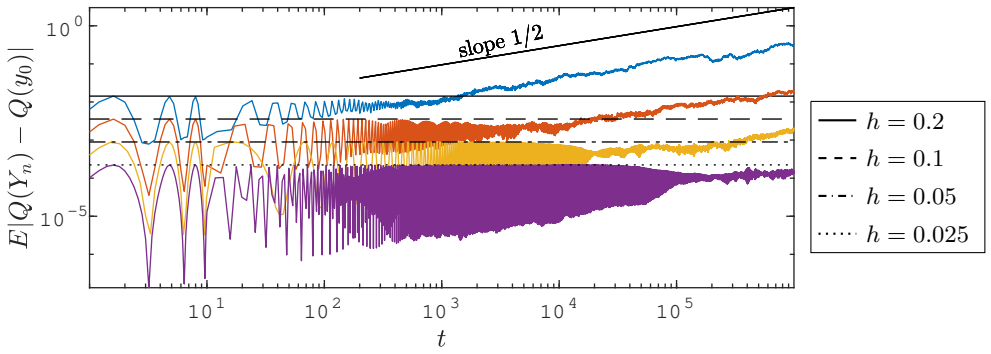

Figure 8: Time evolution of the mean error for the pendulum problem and different values of the time step h. The black lines represent the theoretical estimate given by Theorem 6, while the colored lines represent the experimental results. The mean was computed averaging 20 realisations of the numerical solution.

$\mathbb{R}$, the Störmer–Verlet scheme simplifies to

$$\begin{aligned} v_{n+1/2} &= v_n - \frac{h}{2}\nabla_w Q_2(w_n), \\ w_{n+1} &= w_n + h\nabla_v Q_1(v_{n+1/2}), \\ v_{n+1} &= v_{n+1/2} - \frac{h}{2}\nabla_w Q_2(w_{n+1}). \end{aligned} \tag{128}$$

Hence, in the separable case the Störmer–Verlet scheme is explicit and the evaluation of the flow consists only of three evaluations of the derivatives of Q. We then employ this method both with a fixed time step h and as a basic integrator for the RTS-RK method (with uniformly distributed time steps and $p = 2$), thus computing the posterior distributions $\pi^h(y_0 \mid y_{\text{obs}})$ and $\pi^h_{\text{prob}}(y_0 \mid y_{\text{obs}})$ defined in Section 8, respectively. Moreover, we compute the posterior distribution given by a non-symplectic method, the Heun's scheme, which is a classical second order method. The time step h is varied for the three methods above in order to observe convergence towards the true posterior distribution $\pi(y_0 \mid y_{\text{obs}})$.

We can observe in Fig. 9 that the posterior distributions given by Heun's method are concentrated away from the true value of the initial condition for the larger values of the time step. In fact, Heun's method is not symplectic, and a deviation on the energy Q is produced when integrating in time the dynamical system. Hence, initial conditions with a different energy level with respect to the observation are endowed with a high value of likelihood and the resulting posterior distribution is concentrated far from the true value. This behaviour is corrected using the Störmer–Verlet method thanks to its symplecticity. However, we remark that the posterior distribution for $h = 0.2$ is still concentrated on a biased value of the initial condition, without any indication of this bias given by the posterior's variance. Applying the RTS-RK method together with PMMH instead gives nested posterior distributions whose variance quantifies the uncertainty of the numerical solver. This favourable behaviour is possible thanks to the numerical error quantification of probabilistic methods, which has been already shown in [5,6], together with the good energy conservation properties of the RTS-RK method when a symplectic integrator is used as its deterministic component as proved in Theorem 6.

Appendix

Proof of Lemma 6. Let us first consider $r \geq 2$ and the function $\gamma_r(x) = x^r e^{-r\kappa/x}$, whose first derivative is given by

$$\gamma_r'(x) = rx^{r-2}(x + \kappa)e^{-r\kappa/x}. \tag{129}$$

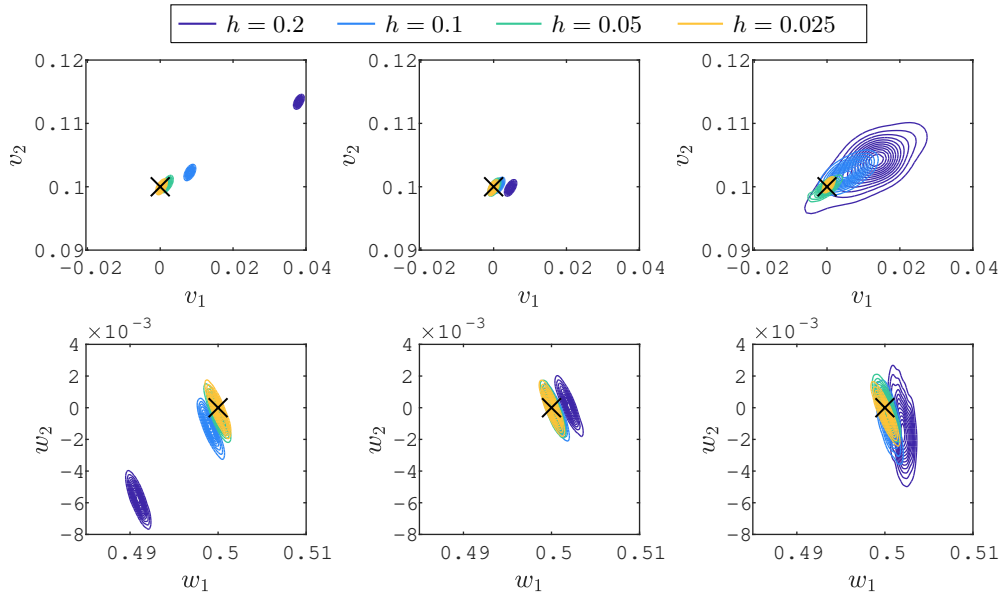

Figure 9: Posterior distributions for the initial position and velocity of the Hénon-Heiles system with different values of $h = \{0.2, 0.1, 0.05, 0.025\}$. First row: initial velocity v_0. Second row: initial position w_0. First column: deterministic Heun's method. Second column: deterministic Störmer–Verlet scheme. Third column: RTS-RK Störmer–Verlet ($p = 2$).

Under Assumption 6 we have for any $t \in [h, H_j]$

$$|\gamma_r'(t)| \leq r(Mh)^{r-2}(Mh + \kappa)e^{-r\kappa/(Mh)}. \tag{130}$$

The fundamental theorem of calculus gives

$$\begin{aligned} |\gamma_r(H_j)| &= \left|\gamma_r(h) + \int_h^{H_j} \gamma_r'(t)\mathrm{d}t\right| \\ &\leq \gamma_r(h) + r(Mh)^{r-2}(Mh + \kappa)e^{-r\kappa/(Mh)}|H_j - h|, \quad \text{almost surely.} \end{aligned} \tag{131}$$

Taking expectation on both sides and as $|\eta_j|^r \leq C\gamma_r(H_j)$ we obtain

$$\mathbb{E}|\eta_j|^r \leq C\big(\gamma_r(h) + rM^{r-2}h^{p+r-3/2}(Mh + \kappa)e^{-r\kappa/(Mh)}\big), \tag{132}$$

which proves the desired as $e^{-r\kappa/x}$ is a growing function of x. Let us now consider $r = 1$. In this case we have for $t \in [h, H_j]$

$$|\gamma_1'(t)| \leq (mh)^{-1}(Mh + \kappa)e^{-\kappa/(Mh)}, \quad \text{almost surely.} \tag{133}$$

Hence, we apply the same reasoning as above and obtain

$$|\gamma_1(H_j)| \leq \gamma_1(h) + (mh)^{-1}(Mh + \kappa)e^{-\kappa/(Mh)}|H_j - h|, \tag{134}$$

which implies the desired result proceeding as above. □

References

[1] A. Abdulle, *Fourth order Chebyshev methods with recurrence relation*, SIAM J. Sci. Comput., 23 (2002), pp. 2041–2054.

[2] A. Abdulle and A. A. Medovikov, *Second order Chebyshev methods based on orthogonal polynomials*, Numer. Math., 90 (2001), pp. 1–18.

[3] C. Andrieu and G. O. Roberts, *The pseudo-marginal approach for efficient Monte Carlo computations*, Ann. Statist., 37 (2009), pp. 697–725.

[4] O. A. Chkrebtii, D. A. Campbell, B. Calderhead, and M. A. Girolami, *Bayesian solution uncertainty quantification for differential equations*, Bayesian Anal., 11 (2016), pp. 1239–1267.

[5] J. Cockayne, C. Oates, T. Sullivan, and M. Girolami, *Probabilistic numerical methods for PDE-constrained Bayesian inverse problems*, AIP Conference Proceedings, 1853 (2017), p. 060001.

[6] P. R. Conrad, M. Girolami, S. Särkkä, A. Stuart, and K. Zygalakis, *Statistical analysis of differential equations: introducing probability measures on numerical solutions*, Stat. Comput., (2016).

[7] M. Dashti and A. M. Stuart, *The Bayesian Approach to Inverse Problems*, in Handbook of Uncertainty Quantification, Springer, 2016, pp. 1–118.

[8] E. Hairer, *Variable time step integration with symplectic methods*, Appl. Numer. Math., 25 (1997), pp. 219–227.

[9] E. Hairer, C. Lubich, and G. Wanner, *Geometric Numerical Integration. Structure-Preserving Algorithms for Ordinary Differential Equations*, Springer Series in Computational Mathematics 31, Springer-Verlag, Berlin, second ed., 2006.

[10] E. Hairer, S. P. Nørsett, and G. Wanner, *Solving Ordinary Differential Equations I. Nonstiff Problems*, vol. 8, Springer Verlag Series in Comput. Math., Berlin, 1993.

[11] E. Hairer and G. Wanner, *Solving ordinary differential equations II. Stiff and differential-algebraic problems*, Springer-Verlag, Berlin and Heidelberg, 1996.

[12] M. Hénon and C. Heiles, *The applicability of the third integral of motion: Some numerical experiments*, Astronom. J., 69 (1964), pp. 73–79.

[13] D. J. Higham and A. M. Stuart, *Analysis of the dynamics of local error control via a piecewise continuous residual*, BIT, 38 (1998), pp. 44–57.

[14] H. Kersting and P. Hennig, *Active uncertainty calibration in Bayesian ODE solvers*, in Proceedings of the 32nd Conference on Uncertainty in Artificial Intelligence (UAI 2016), AUAI Press, 2016, pp. 309–318.

[15] H. Lamba and A. M. Stuart, *Convergence results for the MATLAB* ODE23 *routine*, BIT, 38 (1998), pp. 751–780.

[16] H. C. Lie, T. J. Sullivan, and A. L. Teckentrup, *Random Forward Models and Log-Likelihoods in Bayesian Inverse Problems*, SIAM/ASA J. Uncertain. Quantif., 6 (2018), pp. 1600–1629.

[17] E. N. Lorenz, *Deterministic nonperiodic flow*, J. Atmos. Sci., 20 (1963), pp. 130–141.

[18] G. N. Milstein and M. V. Tretyakov, *Stochastic numerics for mathematical physics*, Scientific Computing, Springer-Verlag, Berlin and New York, 2004.

[19] ——, *Numerical integration of stochastic differential equations with nonglobally Lipschitz coefficients*, SIAM J. Numer. Anal., 43 (2005), pp. 1139–1154.

[20] L. F. Olsen, *An enzyme reaction with a strange attractor*, Phys. Lett. A, 94 (1983), pp. 454 – 457.

[21] M. Schober, D. Duvenaud, and P. Hennig, *Probabilistic ODE solvers with Runge–Kutta means*, in Advances in Neural Information Processing Systems 27, Curran Associates, Inc., 2014, pp. 739–747.

[22] R. D. Skeel and C. W. Gear, *Does variable step size ruin a symplectic integrator?*, Physica, 60 (1992), pp. 311–313.

[23] C. Störmer, *Sur les trajectoires des corpuscules électrisés*, Arch. sci. phys. nat. Genève, 24 (1907), pp. 5–18, 113–158, 221–247.

[24] A. M. Stuart, *Inverse problems: a Bayesian perspective*, Acta Numer., 19 (2010), pp. 451–559.

[25] T. J. Sullivan, *Well-posed Bayesian inverse problems and heavy-tailed stable quasi-Banach space priors*, Inverse Probl. Imaging, 11 (2017), pp. 857–874.

[26] P. van der Houwen and B. P. Sommeijer, *On the internal stage Runge-Kutta methods for large m-values*, Z. Angew. Math. Mech., 60 (1980), pp. 479–485.

[27] L. Verlet, *Computer "experiments" on classical fluids. I. Thermodynamical properties of Lennard-Jones molecules*, Physical Review, 159 (1967), pp. 98–103.